Int J Earth Sci (Geol Rundsch) (2004) 93:782–801
DOI 10.1007/s00531-004-0419-2

ORIGINAL PAPER

U. Teipel · R. Eichhorn · G. Loth · J. Rohrmüller · R. Höll · A. Kennedy

U-Pb SHRIMP and Nd isotopic data from the western Bohemian Massif (Bayerischer Wald, Germany): Implications for Upper Vendian and Lower Ordovician magmatism

Received: 13 May 2004 / Accepted: 26 June 2004 / Published online: 26 August 2004

Abstract U-Pb SHRIMP dating of zircons of metamagmatites from the Bayerischer Wald (Germany) reveals a complex evolution of this section of the Moldanubian Zone exposed in the western Bohemian Massif of the central European Variscan belt. In the south-western part of the Bayerischer Wald Upper Vendian magmatism is constrained by pooled $^{206}Pb/^{238}U$ mean ages of 555±12, 549±7 and 549±6 Ma from metarhyolites and a metabasite. Inherited zircon cores were not observed. Zircon overgrowths, yielding pooled $^{206}Pb/^{238}U$ ages of 316±10 and 319±5 Ma, provide evidence for Variscan metamorphic zircon growth; cathodoluminescence imaging reveals a two-stage metamorphic overprint.
In contrast, Lower Ordovician magmatism and anatexis are documented in the north-eastern parts of the Bayerischer Wald by metagranitoids (480±6, 486±7 Ma), an eclogitic metabasite (481±8 Ma) and a leucosome (491 to 457 Ma). Inherited zircon cores are found in Lower Ordovician metagranitoids and the leucosome, indicating a Palaeoproterozoic-Archaean (ca. 2.7, 2.0 Ga) source region, presumably of Gondwana affinity (West African craton), and documenting Cadomian magmatism (ca. 640 Ma). Post-Cadomian metamorphism is inferred from concordant ages of 433±4 and 431±7 Ma.
Upper Vendian magmatism is assumed at an active continental margin with ensialic back-arc development ($\epsilon_{Nd(t)}$ –3.01 to +1.22); the lack of inherited zircon is due to either derivation from juvenile (?volcanic arc) material or complete isotopic resetting of pre-existing zircon. An active continental margin setting, possibly with some lateral variation (accretion/collision) is envisaged for the Lower Ordovician, producing granitoids, rhyolites and leucosomes ($\epsilon_{Nd(t)}$ -0.5 to -6.27); MORB-type metabasites may be related to ZEV or Mariánské Lázně Complex metabasites. A tentative palaeogeographic reconstruction puts the "Bayerischer Wald" in close relationship with the Habach terrane (proto-Alps), as the "eastern" extension of terranes of the northern Gondwana margin.

Keywords Moldanubian · Bayerischer Wald · Zircon SHRIMP dating · Nd isotopes · Cathodoluminescence

Abbreviations *PA:* Passau area · *HBW:* Hinterer Bayerischer Wald · *SOW:* Southern Oberpfälzer Wald · *KG:* Künisches Gebirge · *CL:* Cathodoluminescence · *ATA:* Armorican terrane assemblage

U. Teipel (✉) · G. Loth
Bayerisches Geologisches Landesamt,
Heßstr. 128, 80797 Munich, Germany
e-mail: ulrich.teipel@gla.bayern.de

R. Eichhorn
Bayerisches Staatsministerium für Umwelt,
Gesundheit und Verbraucherschutz,
Rosenkavalierplatz 2, 81925 Munich, Germany

J. Rohrmüller
Bayerisches Geologisches Landesamt,
Leopoldstr. 30, 95615 Marktredwitz, Germany

U. Teipel · R. Höll
Department für Geo- und Umweltwissenschaften,
LMU München, Luisenstr. 37, 80333 Munich, Germany

A. Kennedy
John de Laeter Centre for Mass Spectrometry,
Curtin University of Technology,
GPO Box U 1987, 6001 Perth, Australia

Introduction

The Moldanubian basement of the Bayerischer Wald represents the western part of the Bohemian Massif in the Variscan belt of central Europe (Fig. 1). The Variscan belt of central Europe is the result of sequential collision of Gondwana-derived crustal fragments during the Variscan orogeny in the Upper to Middle Palaeozoic (Franke et al., 1995; Tait et al., 1997). These crustal fragments are believed to originate from a late Neoproterozoic, Andean-type continental margin at the northern Gondwana margin (Nance and Murphy, 1996). Among the Gondwana-derived terranes in Europe are East-Avalonia, Iberia and

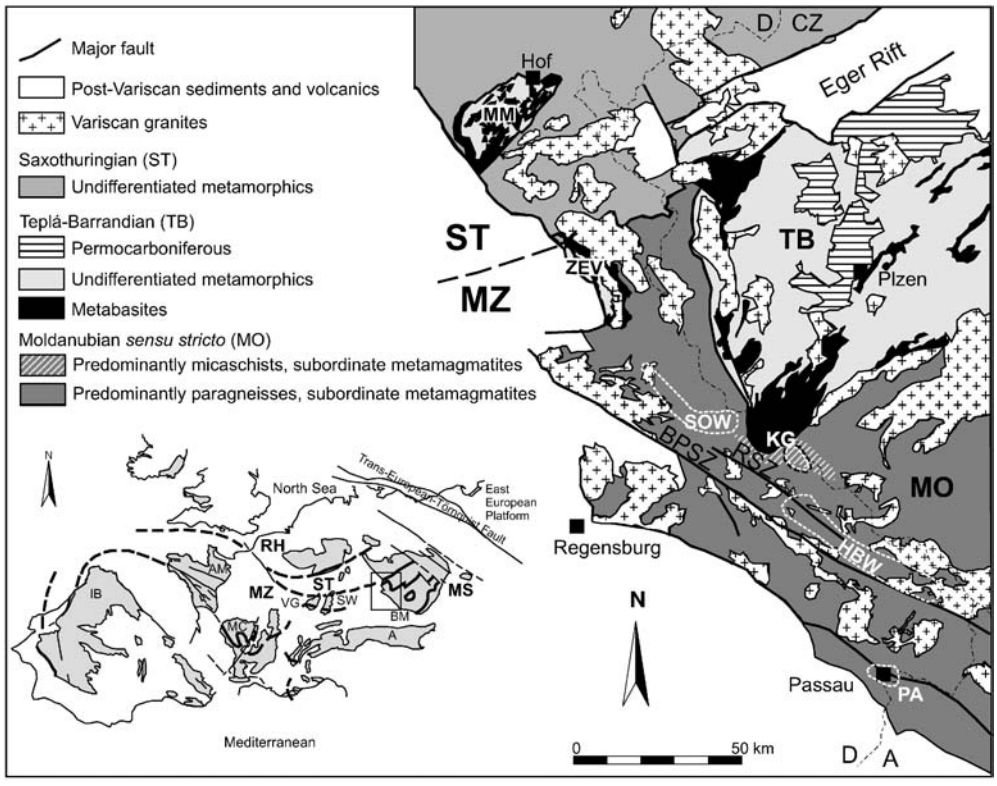

Fig. 1 Geological map of the western Bohemian Massif (modified after Bayer Geol Landesamt, 1996 and Troll, 1967). MM: Münchberg Mass, ZEV: Zone of Erbendorf-Vohenstrauß, BPSZ: Bayerischer Pfahl shear zone, RSZ: Runding shear zone. Sampling areas for SHRIMP and isotopic studies comprise the Passau area (PA), the Hinterer Bayerischer Wald (HBW), the southern Oberpfälzer Wald (SOW), and the Künisches Gebirge (KG; isotopic study only). *Inset*: Variscan belt of Europe (modified after Franke, 1989). RH: Rhenohercynian Zone, ST: Saxothuringian Zone, MZ: Moldanubian Zone, MS: Moravo-Silesian Zone. Variscan massifs are shaded: IB: Iberia, AM: Armorican Massif, MC: Massif Central, VG: Vosges, SW: Schwarzwald, BM: Bohemian Massif, A: Alps.

Cadomia, the latter two being part of the Armorican terrane assemblage (ATA; Tait et al., 1997). In recent years, there has been growing evidence that areas with Avalonian affinities in Europe are not restricted to East-Avalonia but may also be present in parts of the Saxothuringian Zone (Erzgebirge, West-Sudetes) and in the Moravo-Silesian Zone (Friedl, 2000; Kröner and Hegner, 1998; Kröner et al., 1995, 2001). The ATA mainly comprises the Moldanubian Zone (Iberian and Armorican Massifs, Massif Central, Vosges, Schwarzwald, parts of the Bohemian Massif) (Tait et al., 1997) and parts of the Saxothuringian Zone (Schätz et al., 2002). Correlations between the ATA and the proto-Alps (pre-Variscan basement of the Alps) are discussed by von Raumer et al. (2002). Palaeomagnetic data indicate that crustal fragments of the ATA independently separated from Gondwana in the Ordovician between ~ 470 and ~ 440 Ma and drifted towards Laurentia and Baltica (Schätz et al., 2002; Tait et al., 1997, 2000). A wealth of geochronological data exists for most parts of the ATA and neighbouring areas for Neoproterozoic to Ordovician, palaeogeographic reconstructions (Bues et al., 2002; Chen et al., 2000; Dörr et al., 2002; Eichhorn et al., 2001; Friedl, 2000; Hegner and Kröner, 2001; Kemnitz et al., 2002; Kröner and Hegner, 1998; Linnemann et al., 2000; Pin and Marini, 1993; Schaltegger et al.,1997; von Quadt,1997; von Raumer et al., 2002; Zulauf et al., 1997, 1999).

However, data are still lacking for the Moldanubian basement of the Bayerischer Wald, where the limited number of reliable magmatic age data still hampers pre-Variscan palaeogeographic reconstructions. Furthermore, the geotectonic setting is not clear from the small amount of geochemical data available. Thus, the essential aim of this study was to constrain the age and geotectonic setting of metamagmatic rocks from the Bayerischer Wald believed to be pre-Variscan in age. Leucocratic gneisses and, if existent, associated metabasites were sampled in four areas (Fig. 1): the Passau area (PA), the Hinterer Bayerischer Wald (HBW; Bodenmais – Spiegelau – Freyung), the southern Oberpfälzer Wald (SOW; Oberviechtach – Waldmünchen – Rötz) and the Künisches Gebirge (KG; Rittsteig – Lam).

The polyphase evolution of the Moldanubian basement in the Bayerischer Wald, involving original sedimentation/crystallization, subsequent burial, exhumation and decompressional melting, entailing e.g. the presence of inherited zircon cores and partial lead loss, demands age determinations of high spatial resolution. Therefore, SHRIMP analysis of zircons controlled by cathodoluminescence (CL) imaging is used in order to obtain geo-

logically meaningful information on protolith ages and, if documented by zircon growth, on the subsequent evolution. In this paper, for the first time, high-quality protolith ages for pre-Variscan rocks from the Bayerischer Wald are presented. Focus is placed on magmatic formation ages; a tentative model for the palaeogeographic reconstruction of the Moldanubian basement of the Bayerischer Wald is proposed.

Geological setting

The Bayerischer Wald is situated at the south-western margin of the Bohemian Massif, which is part of the Moldanubian Zone of the Variscan belt. In the Bohemian Massif the Moldanubian Zone can be divided into the Teplá-Barrandian and the Moldanubian sensu stricto (in the following referred to as 'Moldanubian') (Franke, 1989). The Bayerischer Wald represents an intensely reworked marginal part of the Moldanubian of the Bohemian Massif; typical structures are NW-SE trending foliations and shear zones (Bayerischer Pfahl shear zone, Runding shear zone). The Moldanubian of the Bayerischer Wald consists of predominantly polyphase metasediments and subordinate metamagmatites, which were intruded by Variscan granitoids (Fig. 1). For the most part, especially in the HBW, metasediments comprise relatively monotonous series of pelitic to psammitic, migmatitic paragneisses with rare intercalations of calcsilicate lenses, leucocratic gneisses and amphibolites (Rohrmüller et al., 1996). In both the southern (PA) and northern (SOW) parts of the Bayerischer Wald lithologies are more varied with frequent intercalations of calcsilicate lenses, marbles, graphite-bearing gneisses, leucocratic gneisses and amphibolites. Similarly varied lithologies are also found in the KG; these metasediments occur as micaschists due to lower metamorphic grade (greenschist-facies; Blümel, 1972). Intercalated leucocratic gneisses comprise volcanogenic (PA, SOW, KG; Bauberger and Unger, 1984; Mielke, 1990, 2002) as well as intrusive metamagmatites (HBW; Bauberger, 1977; Ott, 1988) and leucosomes (SOW/HBW; Teipel, 2003).

Constraints for the sedimentation of metasediment precursors are set in the north-western Bayerischer Wald by minimum ages of ~ 565 Ma (Rb-Sr whole-rock; Grauert et al., 1974), and in the Oberpfälzer Wald by maximum ages of ~ 540 Ma (U-Pb zircon; Teufel, 1988). SHRIMP zircon ages of acid metavolcanics in the SOW and the KG of 472±6 and 474±7 Ma dating magmatic formation are reported by Mielke et al. (1996), implying Lower to Middle Ordovician sedimentation ages for the associated metasediment precursors.

Early phases of the metamorphic evolution of the Bayerischer Wald are indicated by geochronological data (U-Pb zircon and monazite ages, Rb-Sr whole-rock ages) of paragneisses, interpreted as products of metamorphism or anatexis in the early Cambrian at 540–545 Ma, in the Lower Odovician at 490–475 Ma and in the Middle Ordovician at 460–465 Ma (Gebauer et al., 1989; Grauert et al., 1974; Köhler et al., 1989; Teufel, 1988). Scarce eclogite ("Winklarn series") and granulite relics with high-pressure (HP) phases yielding a Sm-Nd mineral-isochrone age of 424±13 Ma (von Quadt and Gebauer, 1993) document HP metamorphism with pressure-temperature (P-T) conditions of 1.2–1.5 GPa and 710–800°C (O'Brien, 1989b). A Devonian (~ 380 Ma; Ihlenfeld et al., 1998; Teufel, 1988) medium-pressure event is represented by relic kyanite and staurolite in paragneisses (Düsing, 1959; Mielke, 1990; Schuster, 1994); P-T conditions were 0.7–0.9 GPa and 530–570°C (Tanner et al., 1993). Characteristic and wide-spread mineral assemblages of migmatitic paragneisses in the Bayerischer Wald comprising cordierite, K-feldspar, ±sillimanite, ±garnet, ±green spinel, reflect the pervasive, Carboniferous low-pressure/high-temperature (LPHT) metamorphism. P-T conditions usually reported are 0.3–0.4 GPa and 640–800°C (Blümel and Schreyer, 1977; Schuster, 1994; Tanner et al., 1993). Kalt et al. (1999, 2000) propose a four-stage clockwise P-T path with a relic, prograde first stage, a second stage of melt-producing biotite dehydration, peak conditions of 0.5–0.7 GPa/850°C and cooling, crystallization in the third stage and a subsequent, retrograde stage with 0.44–0.51 GPa and 770–846°C. Peak conditions of the LPHT metamorphism were reached at 326–316 Ma as shown by U-Pb zircon data (Kalt et al., 2000) and U-Pb monazite data (Grauert et al., 1974; Propach et al., 2000; Teufel, 1988). The timing of cooling is constrained by U-Pb ages of sphene (321 Ma), and Ar-Ar ages of hornblende (322–316 Ma) and biotite (313–309 Ma) (Kalt et al., 2000). For the intrusion of Variscan granites in the Bayerischer Wald U-Pb and Pb-Pb zircon ages range from 330 to 310 Ma (Grauert et al., 1974; Propach et al., 2000; Siebel et al., 2003).

Rock types sampled in the present study comprise metarhyolites, metagranitoids, leucosomes and metabasites (Table 1). Metarhyolites from the PA, SOW and KG are composed of K-feldspar, quartz, plagioclase, biotite, ±garnet, ±sillimanite and ±muscovite; accessories are zircon, ±epidote minerals, ±monazite, ±opaque minerals, ±apatite, ±sphene and rare green spinel. Most PA and SOW metarhyolites contain garnet and/or sillimanite documenting high-grade metamorphic conditions; whereas KG metarhyolites lack garnet/sillimanite consistent with a metamorphic grade below the sillimanite isograd (Blümel, 1972). Leucosomes from the Bodenmais – Waldmünchen area (HBW/SOW) are petrographically similar to metarhyolites; their migmatitic origin is indicated by characteristically low REE contents, high P concentrations and mainly positive Eu anomalies (Teipel, 2003). HBW metagranitoids are characterized by prevalence of plagioclase over K-feldspar and are composed of plagioclase, quartz, K-feldspar, biotite, ±muscovite, ±garnet, accessory zircon, apatite, monazite and opaque minerals. Metabasites from the PA and SOW differ slightly in mineral content: PA metabasites are composed of amphibole, plagioclase, epidote, minor garnet, accessory quartz, apatite, opaque minerals, sphene and zircon. In the SOW, amphibolites and eclogitic amphibolites are composed

Table 1 Compilation of samples analyzed by SHRIMP with short description and geotectonic setting as deduced by geochemistry. R, H: Gauss-Krüger coordinates. Ref.: Petrographical and geochemical references: 1: Bauberger (1977); 2: Bauberger and Unger (1984); 3: Mielke (1990,2002); 4: Ott (1988); 5: Teipel (2003); 6: Troll et al. (1987); 7: Düsing (1959), O'Brien (1989a)

Sample	Locality	Rock name	Geochemistry	Ref.
PA8–2 Metarhyolite	Passau-Hacklberg R: 4607340, H: 5383200	garnet-bearing biotite-K–feldspar gneiss	Rhyodacite; continental and subduction signature; active continental margin	2, 5
PA11–1 Metarhyolite	Haibach (Austria), SW Passau R: 4611000, H: 538 2000	biotite-bearing K–feldspar gneiss	Rhyolite; continental and subduction signature; active continental margin	2, 5
PA9–3 Metabasite	Haibach (Austria), SW Passau R: 4610380, H: 5382150	epidote-bearing amphibolite	Sub-alkaline basalt; enriched MORB; ensialic back arc	2, 5
HBW1–1 Metagranitoid	S Spiegelau R: 4600075, H: 5419430	biotite-plagioclase gneiss	Granodiorite; continental and subduction signature; active continental margin	1, 4, 5
HBW31–2 Metagranitoid	2.5 km E Bodenmais R: 4583350, H: 5437220	garnet-bearing biotite-plagioclase gneiss	Granodiorite; continental and subduction signature; active continental margin	5, 6
HBW11–1 Leucosome	Böbrach 5.5 km SE Bodenmais R: 4576070, H: 5434480	sillimanite-garnet-bearing biotite-K–feldspar gneiss	Rhyolitic composition; low REE, TiO_2, Zr, Hf, Th; high P ?active continental margin, accretion/collision	3, 5
SOW33–6 Metabasite	Hermannsried, Oberviechtach R: 4529675, H: 5484225	eclogitic amphibolite	basalt; enriched to normal MORB; ?continental rift, oceanic	7

of amphibole, plagioclase, pyroxene, epidote, ±garnet, ±quartz and accessory apatite, sphene, opaque minerals and rare zircon. In the Oberviechtach – Winklarn area amphibolites, eclogitic amphibolites and serpentinites occur as small bodies and are interpreted as partly retrogressed HP relics (O'Brien, 1989b).

Analytical methods

SHRIMP dating of zircon

The samples comprised 3–10 kg of fresh material. Mineral fractions for isotopic analyses were processed through conventional mineral separation techniques, including a Wilfley table, heavy liquids and a Frantz isodynamic separator. Final mineral separates consisted of handpicked, top-quality zircon grains.

Zircon grains from the sample and pieces of the CZ3 standard zircon (Pidgeon, 1997) are mounted and polished in a 24-mm diameter epoxy disc and gold-coated. The zircons were photographed and examined for internal structures with a Zeiss DSM 960A scanning electron microprobe in cathodoluminescence (CL) mode on the polished and gold-coated mounts at the Department für Geo- und Umweltwissenschaften (Ludwig-Maximilians-Universität München). The CL information was obtained prior to the SHRIMP analyses, in order to select appropriate zircons for analysis, to place the ion beam without straddling different zones within the same grain, and to avoid zones which may be typical for zircon domains with disturbed U-Pb systems (Pb loss). CL imaging of the internal structure of the analyzed spot also provides important information for the interpretation of the obtained ages. After CL imaging the zircons were analyzed using the SHRIMP II ion microprobe; the diameter of the analyzed spot was 25 µm. Data reduction was performed with Krill (developed by Peter Kinny, Curtin University, Perth), using the methods of Compston et al. (1984) for common Pb correction. The calculation of $^{206}Pb/^{238}U$ ages is based on the assumption that the bias of the measured $^{206}Pb^+/^{238}U^+$ ratio relative to the true ratio can be described by the same power law relationship (Claoué-Long et al., 1995) between $^{206}Pb^+/^{238}U^+$ and UO^+/U^+ for both the CZ3 standard zircon and the unknown zircon analysis. The uncertainty of the $^{206}Pb/^{238}U$ age of the unknown zircon includes the uncertainty of the $^{206}Pb^+/^{238}U^+$ ratio of the standard. For this reason, in any analytical session every third or fourth analysis is performed on the standard zircon. Reproducibility for the 'standard' Pb/U ratio ranged between ±1.02 and ±1.11% for the SHRIMP sessions. The concentrations of U, Th and Pb are calculated using a similar approach to that used for the calculation of Pb/U ratios, with the 'unknown' referenced to the standard with known U, Th and Pb concentrations (Claoué-Long et al., 1995; Compston et al., 1984; Williams et al., 1996). Uncertainty (1σ) of concentration determination is ±5% for U and Pb, and ±3% for Th (Kennedy, 2000).

Uncertainties (1σ) cited for individual analyses include errors from counting statistics, common ^{208}Pb or ^{204}Pb correction, and U-Pb calibration error based on reproducibility of U-Pb measurements of the standard. Mean ages of pooled analyses were calculated with Plonk (developed by Peter Zeitler, Australian National University, Canberra und David Nelson, Curtin University, Perth) and are quoted at the 95% confidence level. The statistical significance of a mean age is given by χ^2; χ^2 = ca. 1 indicates that the pooled analyses form one population and that scatter is due to analytical and not geological factors. Concordia-intercept ages are at the 95% confidence level; they have been calculated with Isoplot/Ex 2.49 (Ludwig, 2001). If not otherwise indicated, individual ages are quoted as $^{206}Pb/^{238}U$ ages. The $^{206}Pb/^{238}U$ uncertainty is generally the smallest uncertainty, because $^{206}Pb/^{238}U$ ages for SHRIMP analyses of Palaeozoic zircons are usually more precise than $^{207}Pb/^{235}U$ and $^{207}Pb/^{206}Pb$ ages, due to the lower abundance of ^{207}Pb as compared to ^{206}Pb in such zircons. In case of high U content the $^{207}Pb/^{206}Pb$ age is also given and discussed. Apparent ages with concordance ($100\times(^{206}Pb/^{238}U$ age)/($^{207}Pb/^{206}Pb$ age)) of 97 to 103% are regarded as concordant. Decay constants used are those recommended by the IUGS (Steiger and Jäger, 1977). The terminology of periods and epochs quoted herein follows the chronostratigraphic time-scales of Gradstein and Ogg (1996) for the Phanerozoic, Webby et al. (2001) for the Ordovician and Remane et al. (2000) for the Precambrian. The term 'Vendian' is used as a synonym for the 'Terminal Proterozoic System', informally called 'Neoproterozoic III'.

Sm-Nd analyses

Sm-Nd isotope analyses were carried out in the Isotope Laboratory of the Department für Geo- und Umweltwissenschaften, LMU München. About 100 mg whole-rock powder were spiked with a ^{84}Sr-^{149}Sm-^{145}Nd combi-spike, mixed with HF-HNO_3 and decomposed in PTFE bombs by heating at 180°C for one week. Decomposition of refractory phases was ensured by a second step of heating in PTFE bombs with HF at 180°C for one week. Separation of REE, Nd and Sm involved standard procedures using quartz columns with resin DOWEX AG 50W-X8 and PTFE powder coated with HDEHP, respectively, as cation-exchange media. Total procedural blanks were 95 pg Nd and <50 pg Sm. Isotope ratios were measured using a Finnigan MAT 261 mass spectrometer equipped with one fixed and four variable collectors. Nd analyses were done in dynamic multicollector mode. Isotope ratios were normalized to $^{152}Sm/^{147}Sm = 1.78308$ (Wasserburg et al., 1981) and $^{146}Nd/^{144}Nd = 0.7219$ (O'Nions et al., 1977). During the course of this study, analyses of the Ames Nd standard yielded $^{143}Nd/^{144}Nd = 0.512142 \pm 12$ (2σ, $n = 6$). Based on multiple analyses of international rock standards and replicate analyses a reproducibility (2σ) of 0.005% for $^{143}Nd/^{144}Nd$ and 0.5% for $^{147}Sm/^{144}Nd$ is assumed.

Results

Th-U chemistry and internal structures of zircons

The Th and U concentrations of zircon domains analyzed by SHRIMP are shown in Fig. 2. Domains of zircon grains that show oscillatory zoning have been interpreted to reflect magmatic growth. Th/U ratios of oscillatory zoned domains from zircons of leucocratic metamagmatites range from 0.47 to 0.95; this range includes the values from structureless, inner zones (0.6–0.78) (denoted as 'sl' in Fig. 3b, c). The range of Th/U ratios is higher than values generally accepted as the lower limit of magmatic values (Th/U >0.3; Rubatto et al., 2001; Schaltegger et al., 1999; Vavra et al., 1999), but is in good agreement with values (Th/U >0.5) reported by Brown and Fletcher (1999) for non-metamorphic, quaternary rhyolite zircons. Zircons with high-CL inner zones, occasionally with relic oscillatory zoning, (Fig. 3a, d; samples PA8-2, HBW1-1, HBW31-2) have Th/U ratios of 0.33–0.74 interpreted as reflecting a magmatic origin, partly affected by secondary processes. Oscillatory zoned and structureless zircon domains from a metabasite (PA9–3) have high Th/U ratios of 1.02 to 1.89 typical for magmatic zircon from mafic rocks (Heaman et al., 1990).

Unzoned, medium- to high-CL overgrowths and rims (Fig. 3a, b; PA8-2, PA11-1) have Th/U ratios <0.1, often <0.01, characteristic for metamorphic zircon (Rubatto et al., 1999; Schaltegger et al., 1999; Williams et al., 1996).

A number of zircons show faded oscillatory zoning (Fig. 3b, c, e-g), with Th/U ratios intermediate between metamorphic and magmatic values (0.17 to 0.49). Fading of magmatic structures may result from thermal (amphibolite- or eclogite-facies) events, yielding metamorphic ages (Rubatto, 2002; Schaltegger et al., 1999; Vavra et al., 1996), or it may be attributed to solid-state, closed-system annealing processes during or directly after zircon crystallization in a slowly cooling magma (Pidgeon et al., 1998) or recrystallization by (late-stage) magmatic fluids/melts (Nemchin and Pidgeon, 1997).

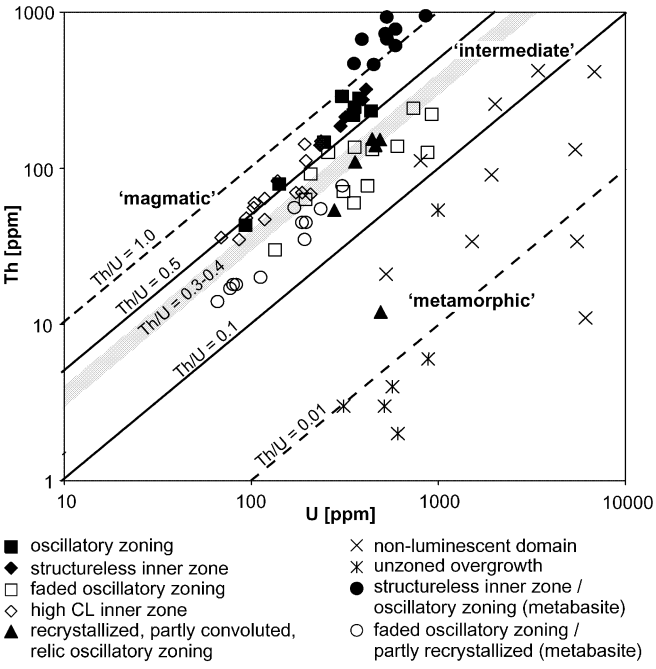

Fig. 2 Th and U concentrations of different internal zircon CL structures. Zircons investigated are from leucocratic gneisses if not mentioned otherwise. Relevant Th/U ratios are included for comparison: 1.0 – lower limit for magmatic zircon from mafic rocks; 0.3–0.4 – generally accepted lower limits for magmatic zircon; 0.1 – upper limit for metamorphic zircon (Heaman et al., 1990; Rubatto, 2002; Rubatto et al., 2001; Schaltegger et al., 1999; Vavra et al., 1999). Oscillatory zoned (magmatic) zircons from leucocratic metamagmatites investigated in the present study have Th/U $\geq$ 0.5; zircons with faded primary structures have Th/U ratios intermediate between 'magmatic' and 'metamorphic' values (0.5–0.1) interpreted to reflect annealing/recrystallization of originally magmatic zircon

Some of the studied zircons with non-luminescent zones have extremely high U contents of 1495–6833 ppm (samples HBW1–1, HBW31-2, HBW11-1). In these zircons U content and concordance correlate with 95% probability (n = 10; correlation coefficient = 0.6505); zircons with the highest U contents being reversely discordant. In contrast, zircon domains with U <1000 ppm show no such correlation. Due to metamictization high-U zircons can be subject to Pb loss, normally yielding discordant data points. In the studied high-U zircons increasing concordance and reverse discordance (i.e. an apparent Pb gain or U loss) correlated with increasing U content is observed. On the basis of microstructural investigations of high-U zircons McLaren et al. (1994) conclude that measurement of apparently higher Pb concentrations and thus overestimation of the Pb/U ratio is caused by sputtering effects during SHRIMP analysis due to changes in the microstructure of high-U zircons. It is concluded that for high-U zircons the apparent $^{207}Pb/^{206}Pb$ age is more significant than $^{206}Pb/^{238}U$ and $^{207}Pb/^{235}U$ ages, probably providing the best estimate for a geologically meaningful age.

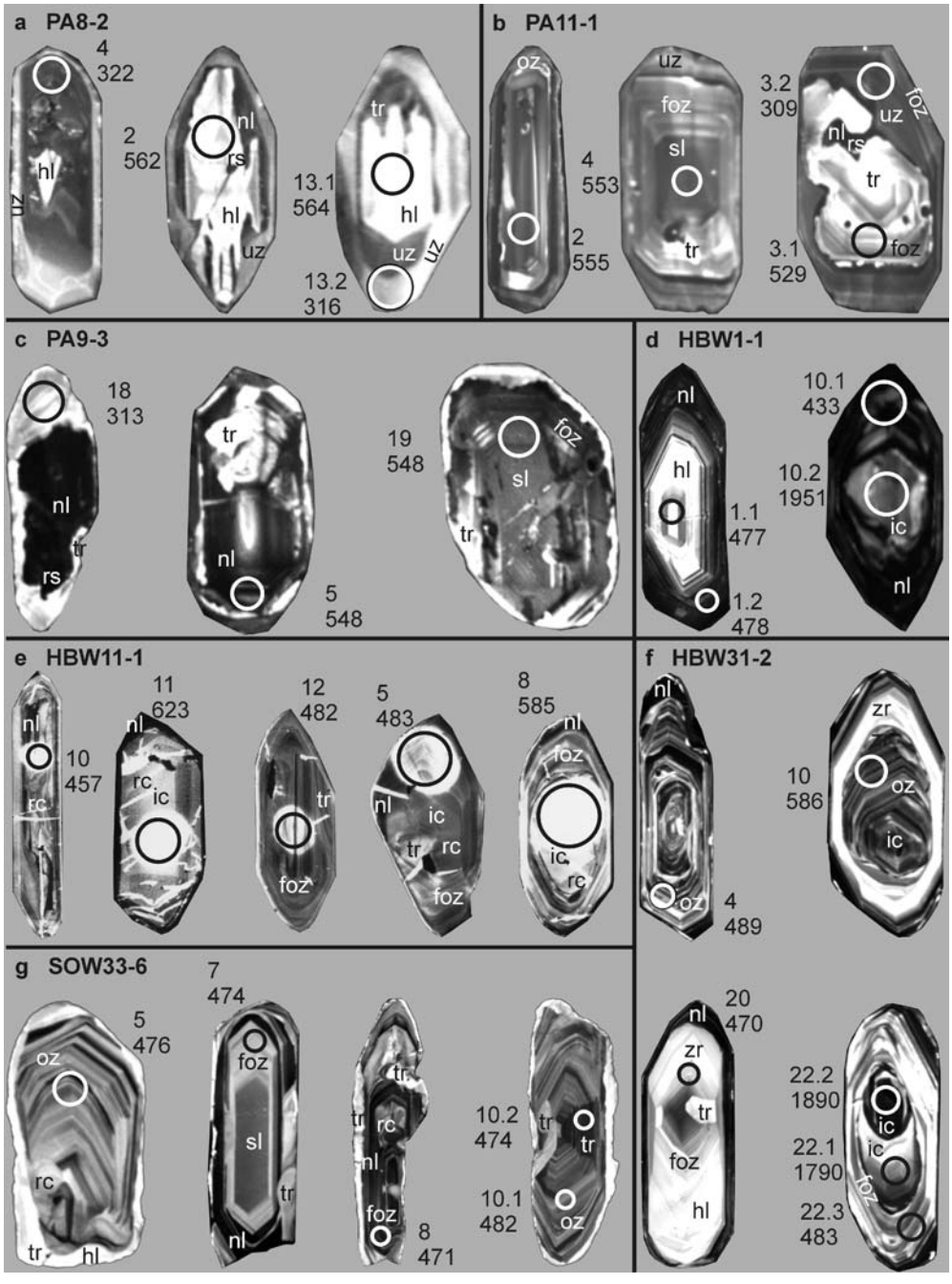

Fig. 3 Cathodoluminescence images of zircons analyzed by ion-microprobe. Spot locations and numbering as well as $^{206}Pb/^{238}U$ SHRIMP ages in Ma are indicated. Radius of the circle indicating the spot location analyzed by SHRIMP corresponds to 25 µm. Abbreviations: ic – inherited core; oz – oscillatory zoning; sl – structureless inner zone; foz – faded oscillatory zoning; uz – unzoned overgrowth; nl – non-luminescent; hl – high CL; rc – recrystallization; zr – zone-controlled recrystallization; tr – transgressive recrystallization; rs – resorbed surface. a Metarhyolite PA8-2; b Metarhyolite PA11-1; c Metabasite PA9-3; d Metagranitoid HBW1–1; e Leucosome HBW11-1; f Metagranitoid HBW31-2; g Metabasite SOW33-6

CL-controlled SHRIMP dating of zircon

Analytical results from SHRIMP analyses of zircons are listed in Table 2.

Zircons of *metarhyolite PA8-2* are mostly euhedral, and only rarely corroded. CL images (Fig. 3a) reveal complex internal structures: euhedral to subhedral cores with extremely high CL and sporadic relics of oscillatory zoning are surrounded by two distinct rims. Inner rims are dark or non-luminescent and may show heterogeneous internal structures with curved boundaries, representing fluid-related reaction fronts. In places, non-luminescent inner rims resorb and intrude into cores. Outer rims are usually thin or irregular with medium to high CL. Rarely, there are recrystallized relics of oscillatory zoning.

Five of six analyzed cores yield a pooled $^{206}Pb/^{238}U$ age of 555±12 Ma (Fig. 4a). Relics of planar oscillatory zoning in high-CL cores and Th/U ratios between 0.40 and 0.58 point to some overprint of originally magmatic zircon. One discordant core analysis (spot 5.1; Fig. 4a) with an apparent $^{206}Pb/^{238}U$ age of 493±9 Ma was not included in the calculation of the mean age.

Rims have 311–880 ppm U, low Th concentrations of 2–6 ppm, and consequently extremely low Th/U ratios <0.01. The apparent ages of inner rims range from 318±3 to 324±4 Ma. Outer rims were too small to place the ion

Table 2 Ion-microprobe analytical results for zircons from the Bayerischer Wald. f206% = 100x(common ^{206}Pb/total ^{206}Pb). Cor = correction method for common Pb: 4 on ^{204}Pb concentration, 8 on ^{208}Pb concentration. Conc = %concordance = 100x(206/238 age)/(207/206 age). Spot description: c: core, rd: rounded, r: rim, z: zone, i: inner, o: outer; for internal structure abbreviations see Fig. 3

Grain	Spot	U	Th	Th/U	Pb	f206%	Ratios corrected for common Pb						Apparent age [Ma]						Cor	Conc
	Description	[ppm]	[ppm]		[ppm]		$^{206}Pb/^{238}U$	±1σ	$^{207}Pb/^{235}U$	±1σ	$^{207}Pb/^{206}Pb$	±1σ	$^{206}Pb/^{238}U$	±1σ	$^{207}Pb/^{235}U$	±1σ	$^{207}Pb/^{206}Pb$	±1σ		[%]
PA8–2 Metarhyolite																				
2	c; hi CL	86	35	0.40	8	0.015	0.0910	15	0.729	67	0.05811	518	562	9	556	40	534	196	4	105
3	c; hi CL	118	64	0.54	11	0.007	0.0876	13	0.706	43	0.05842	331	541	8	542	25	545	124	4	99
4	ir; uz	880	6	0.007	41	0.001	0.0513	6	0.379	6	0.05363	55	322	3	326	4	356	23	8	91
5.1	c; hi CL	69	36	0.52	6	<0.001	0.0795	15	0.687	26	0.06266	194	493	9	531	16	697	66	4	71
5.2	or + ir; uz	311	3	0.008	14	0.002	0.0500	6	0.362	8	0.05260	92	314	4	314	6	312	40	8	101
6	ir; uz	569	4	0.006	27	0.003	0.0515	6	0.373	7	0.05254	69	324	4	322	5	309	30	8	105
9	c; hi CL	94	48	0.51	9	0.004	0.0899	14	0.727	45	0.05866	342	555	8	555	27	554	128	4	100
13.1	c; hi CL	104	60	0.58	10	0.003	0.0914	14	0.749	45	0.05947	333	564	8	568	26	584	122	4	96
13.2	or; uz + ir; nl	516	3	0.007	24	0.002	0.0503	6	0.365	7	0.05271	70	316	4	316	5	316	30	4	100
14.1	c; hi CL	103	56	0.54	10	0.002	0.0902	14	0.747	50	0.06007	380	557	8	567	29	606	137	4	92
14.2	ir; uz	607	2	0.004	28	0.001	0.0505	6	0.368	6	0.05280	65	318	3	318	5	320	28	8	99
PA9–3 Metabasite																				
1	c; relic foz, rc	530	929	1.75	62	0.002	0.0852	9	0.687	14	0.05848	92	527	6	531	8	548	34	4	96
2.1	c; sl	591	609	1.03	61	0.001	0.0887	10	0.724	14	0.05917	88	548	6	553	8	573	32	4	96
2.2	c; sl + nl	857	1024	1.19	91	0.002	0.0848	9	0.672	11	0.05744	68	525	5	522	7	509	26	4	103
5	c; foz	670	1268	1.89	84	0.003	0.0887	10	0.706	14	0.05771	91	548	6	542	8	519	34	4	106
6	c; foz + nl	590	777	1.32	63	0.003	0.0833	9	0.650	13	0.05664	87	516	5	509	8	478	34	4	108
7	c; sl + foz	777	1281	1.65	95	0.006	0.0887	9	0.709	15	0.05795	101	548	6	544	9	528	38	4	104
9	c; oz, partly hi CL	532	673	1.27	60	0.005	0.0887	10	0.706	17	0.05776	114	548	6	543	10	521	43	4	105
10	c; foz	391	670	1.71	49	0.004	0.0909	10	0.724	19	0.05780	132	561	6	553	11	522	50	4	107
11	c; sl, hi CL centre	451	462	1.02	45	0.002	0.0823	9	0.655	17	0.05769	128	510	6	511	11	518	49	4	99
16	c; hi CL + ir; nl	308	371	1.21	32	0.008	0.0823	10	0.633	24	0.05582	196	510	6	498	15	445	78	8	115
17	oc; foz	354	468	1.32	41	0.010	0.0886	10	0.689	24	0.05639	179	547	6	532	15	468	70	4	117
18	r; hi CL, relic foz	134	30	0.22	7	0.006	0.0498	8	0.359	15	0.05233	187	313	5	312	11	300	82	8	104
19	oc; foz + ic; sl	521	728	1.40	60	0.002	0.0888	10	0.700	14	0.05716	91	548	6	539	9	498	35	4	110
PA11–1 Metarhyolite																				
1.1	c iz; sl	236	149	0.63	24	0.012	0.0895	11	0.728	24	0.05900	171	553	7	555	14	567	63	8	97
1.2	r; foz	924	221	0.24	44	0.007	0.0490	5	0.353	7	0.05220	79	309	3	307	5	294	35	8	105
2	c; foz	377	280	0.74	38	0.003	0.0900	10	0.725	20	0.05843	136	555	6	554	12	546	51	8	102
3.1	c; foz, partly hi CL	208	92	0.44	19	0.011	0.0855	11	0.707	21	0.05999	154	529	6	543	13	603	56	8	88
3.2	r; uz	418	77	0.18	20	0.011	0.0491	6	0.357	9	0.05277	114	309	4	310	7	319	49	8	97
4	c iz; sl	411	321	0.78	42	0.005	0.0896	11	0.744	22	0.06027	152	553	6	565	13	613	55	8	90
5	c iz; sl, partly tr	300	186	0.62	29	0.007	0.0861	11	0.671	20	0.05656	148	532	6	521	12	474	58	8	112
6	c; oz	305	289	0.95	32	0.007	0.0886	11	0.712	25	0.05827	182	547	6	546	15	540	69	8	101
7.1	c iz; sl	318	213	0.67	31	0.006	0.0865	10	0.694	21	0.05822	156	535	6	535	13	538	59	8	99
7.2	or; uz + ir; nl	995	54	0.05	48	0.005	0.0519	6	0.381	7	0.05321	63	326	3	328	5	338	27	8	97
8.1	c iz; sl	394	275	0.70	39	0.009	0.0876	11	0.719	21	0.05958	146	541	7	550	12	588	53	8	92
8.2	or; uz + ir; nl	877	126	0.14	41	0.008	0.0499	5	0.361	7	0.05256	75	314	3	313	5	310	32	8	101
10	c; foz, partly hi CL	352	219	0.62	34	0.004	0.0889	11	0.733	22	0.05976	152	549	6	558	13	595	55	4	92
11	c iz; sl, partly hi CL	240	143	0.60	23	0.021	0.0851	12	0.676	25	0.05758	188	526	7	524	15	514	72	8	102
13	ir; nl + c	1513	34	0.02	73	0.002	0.0527	5	0.391	5	0.05382	44	331	3	335	4	363	18	8	91
14	or; uz + ir; nl	736	242	0.33	38	0.009	0.0509	6	0.366	8	0.05212	95	320	3	317	6	291	42	8	110
16	c; foz, partly hi CL	357	246	0.69	36	0.002	0.0901	10	0.734	23	0.05909	159	556	6	559	13	570	59	4	98
HBW11–1 Leucosome																				
1.1	c; rc, partly nl	278	69	0.25	54	0.000	0.1883	20	2.583	37	0.09947	78	1112	11	1296	10	1614	15	4	69
1.2	or; rc + ir; foz	491	12	0.02	36	0.001	0.0791	8	0.611	9	0.05605	51	491	5	484	6	454	20	8	108
4	or + ir; rc	475	148	0.31	36	<0.001	0.0758	8	0.600	10	0.05734	70	471	5	477	7	505	27	8	93
5	r; foz	278	54	0.19	21	0.001	0.0778	9	0.608	18	0.05672	151	483	5	482	12	481	59	4	100
6	c rd; foz, partly nl	349	545	1.56	44	0.003	0.0938	10	0.779	17	0.06026	104	578	6	585	10	613	37	4	94
8	c rd; rc, patchy	175	102	0.58	18	0.002	0.0950	12	0.798	30	0.06088	204	585	7	596	17	635	72	4	92
10	c; rc, convolute	461	145	0.31	34	0.005	0.0735	8	0.577	15	0.05694	125	457	5	462	10	489	48	4	93
11	c; rc, planar	112	35	0.31	12	0.006	0.1015	14	0.871	48	0.06223	320	623	8	636	26	682	110	4	91
12	c; foz	455	149	0.33	35	0.002	0.0776	8	0.588	11	0.05492	76	482	5	470	7	409	31	8	118
13	iz; relic foz + rc	525	21	0.04	37	0.005	0.0754	8	0.591	9	0.05683	59	468	5	471	6	485	23	8	97
14	iz; nl	6833	415	0.06	552	0.001	0.0851	8	0.658	7	0.05610	17	526	5	513	4	456	7	4	115
15.1	c; rc, convolute	359	110	0.31	38	0.004	0.1039	11	0.873	19	0.06094	107	637	7	637	10	637	38	4	100
15.2	r; nl, foz	6114	11	0.002	453	<0.001	0.0815	8	0.634	7	0.05641	14	505	5	498	4	469	6	4	108
16	oz; nl, relic foz	5517	34	0.01	338	<0.001	0.0673	7	0.515	6	0.05547	18	420	4	422	4	431	7	4	97
17	c rd; sl	684	181	0.27	237	0.003	0.3337	34	5.591	64	0.12151	48	1856	17	1915	10	1978	7	4	94
18	c rd; rc, patchy	2977	33	0.01	211	0.004	0.0766	8	0.635	8	0.06019	37	476	5	499	5	610	13	4	78

Table 2 (continued)

Grain	Spot	U	Th	Th/U	Pb	f206%	Ratios corrected for common Pb						Apparent age [Ma]						Cor	Conc
	Description	[ppm]	[ppm]		[ppm]		$^{206}Pb/^{238}U$	±1σ	$^{207}Pb/^{235}U$	±1σ	$^{207}Pb/^{206}Pb$	±1σ	$^{206}Pb/^{238}U$	±1σ	$^{207}Pb/^{235}U$	±1σ	$^{207}Pb/^{206}Pb$	±1σ		[%]
HBW1–1 Metagranitoid																				
1.1	iz; hi CL	196	112	0.57	16	0.003	0.0768	10	0.593	20	0.05594	164	477	6	473	13	450	65	8	106
1.2	oz; nl	2014	258	0.13	147	0.001	0.0770	7	0.606	7	0.05707	34	478	4	481	4	494	13	8	97
2.1	oz; nl	3414	421	0.12	249	0.004	0.0763	7	0.591	6	0.05621	26	474	4	472	4	461	10	8	103
2.2	iz; hi CL, rc	138	83	0.61	11	0.002	0.0738	10	0.597	31	0.05871	282	459	6	475	20	556	105	4	82
3.1	c; relic foz, partly tr	166	65	0.39	17	0.002	0.0999	12	0.849	23	0.06164	137	614	7	624	12	662	48	8	93
3.2	r; nl	803	112	0.14	63	0.021	0.0764	7	0.623	10	0.05914	63	475	4	492	6	572	23	8	83
5	iz; foz, partly hi CL	141	79	0.56	12	0.002	0.0766	10	0.617	23	0.05843	194	476	6	488	14	546	72	8	87
6.1	iz; hi CL + nl centre	193	143	0.74	16	<0.001	0.0769	10	0.621	13	0.05856	95	478	6	490	8	551	36	8	87
6.2	iz; hi CL	187	70	0.37	15	0.004	0.0780	10	0.606	18	0.05629	142	484	6	481	11	464	56	8	104
8.1	c; relic foz	310	308	0.99	36	0.001	0.0970	11	0.783	24	0.05855	160	597	6	587	14	550	60	8	108
8.2	r; nl	5391	132	0.02	430	<0.001	0.0872	8	0.684	7	0.05688	17	539	5	529	4	487	6	8	111
9.1	oz; foz, partly nl	344	35	0.10	25	0.001	0.0785	9	0.622	11	0.05744	78	487	5	491	7	509	30	8	96
9.2	iz; relic foz, partly nl	311	71	0.23	24	0.002	0.0794	9	0.619	13	0.05649	94	493	5	489	8	471	37	8	105
10.1	r; relic foz, partly nl	605	138	0.23	43	0.011	0.0694	7	0.533	18	0.05568	172	433	4	434	12	439	69	4	98
10.2	c; rc	281	128	0.45	114	0.008	0.3534	37	8.345	102	0.17126	90	1951	18	2269	11	2570	9	8	76
11	oz; foz	245	147	0.60	21	<0.001	0.0792	9	0.638	19	0.05841	151	491	6	501	12	545	57	8	90
12	iz; hi CL	207	68	0.33	16	0.001	0.0760	9	0.605	16	0.05777	129	472	6	481	10	521	49	8	91
13	iz; relic foz, partly hi CL	195	63	0.32	15	0.003	0.0775	10	0.599	17	0.05603	131	481	6	477	11	453	52	8	106
14	iz; hi CL, relic foz	118	47	0.40	10	0.003	0.0786	11	0.601	23	0.05546	184	488	7	478	14	431	74	8	113
HBW31–2 Metagranitoid																				
1	iz; foz	258	126	0.49	21	0.004	0.0786	10	0.603	19	0.05566	151	488	6	479	12	439	60	8	111
2	ir; foz	444	132	0.30	33	0.006	0.0743	8	0.578	13	0.05647	97	462	5	463	8	471	38	8	98
4	iz; oz, partly nl + hl zones	437	233	0.53	37	0.006	0.0788	9	0.616	15	0.05668	117	489	6	487	10	479	46	8	102
6.1	c rd; foz	341	154	0.45	34	0.005	0.0954	11	0.797	20	0.06061	129	587	7	595	12	625	46	8	94
6.2	ir; hi CL, relic foz	88	65	0.74	8	0.017	0.0775	13	0.643	40	0.06014	345	481	8	504	25	609	124	8	79
8.1	iz; hi CL, relic foz	173	70	0.40	14	0.009	0.0794	12	0.609	42	0.05565	369	492	7	483	27	438	148	4	112
8.2	oz; foz	354	60	0.17	27	0.003	0.0787	9	0.624	13	0.05749	93	489	6	492	8	510	35	8	96
8.3	or; nl	1922	91	0.05	144	0.001	0.0811	8	0.639	8	0.05718	34	503	5	502	5	498	13	8	101
10	c; oz	463	166	0.36	43	0.002	0.0911	10	0.748	15	0.05952	92	562	6	567	9	586	33	8	96
20	iz; oz, partly hi CL zones	93	43	0.47	8	0.014	0.0756	12	0.610	33	0.05845	286	470	7	483	21	547	107	8	86
22.1	c rd; relic foz, partly hi CL	325	345	1.06	129	0.002	0.3201	37	5.373	95	0.12172	147	1790	18	1881	15	1982	21	8	90
22.2	c rd; nl	1495	190	0.13	509	0.001	0.3407	35	5.753	66	0.12249	49	1890	17	1939	10	1993	7	8	95
22.3	r; foz	356	136	0.38	28	0.006	0.0777	9	0.603	15	0.05626	119	483	5	479	10	463	47	8	104
SOW33–6 Metabasite																				
2	c; foz	83	18	0.22	6	0.009	0.0738	13	0.609	26	0.05987	224	459	8	483	17	599	81	8	77
4	c; foz	196	45	0.23	16	0.008	0.0795	10	0.605	18	0.05520	137	493	6	480	11	420	56	8	117
5	c; foz	80	18	0.23	6	0.024	0.0766	13	0.609	29	0.05770	249	476	8	483	19	518	95	8	92
6	c; foz	193	35	0.18	15	0.007	0.0785	10	0.608	18	0.05619	135	487	6	482	11	460	53	8	106
7	oc; foz	66	14	0.22	5	0.027	0.0763	14	0.593	32	0.05633	279	474	8	473	21	466	110	8	102
8	c; foz, partly nl	235	55	0.23	18	0.012	0.0758	10	0.583	17	0.05582	135	471	6	466	11	445	54	8	106
9.1	oc; foz	112	20	0.18	9	0.016	0.0802	12	0.657	27	0.05940	211	497	7	513	16	582	77	8	85
9.2	ic; nl	306	77	0.25	24	0.006	0.0779	9	0.596	15	0.05552	116	484	6	475	10	433	46	8	112
10.1	c; foz	77	17	0.22	6	0.032	0.0777	13	0.639	34	0.05966	292	482	8	502	21	591	106	8	82
10.2	c; foz, tr	170	56	0.33	14	0.012	0.0763	10	0.615	21	0.05847	172	474	6	487	13	547	64	8	87
12	oc; foz	187	45	0.24	15	0.008	0.0788	10	0.618	18	0.05691	135	489	6	489	11	488	53	8	100

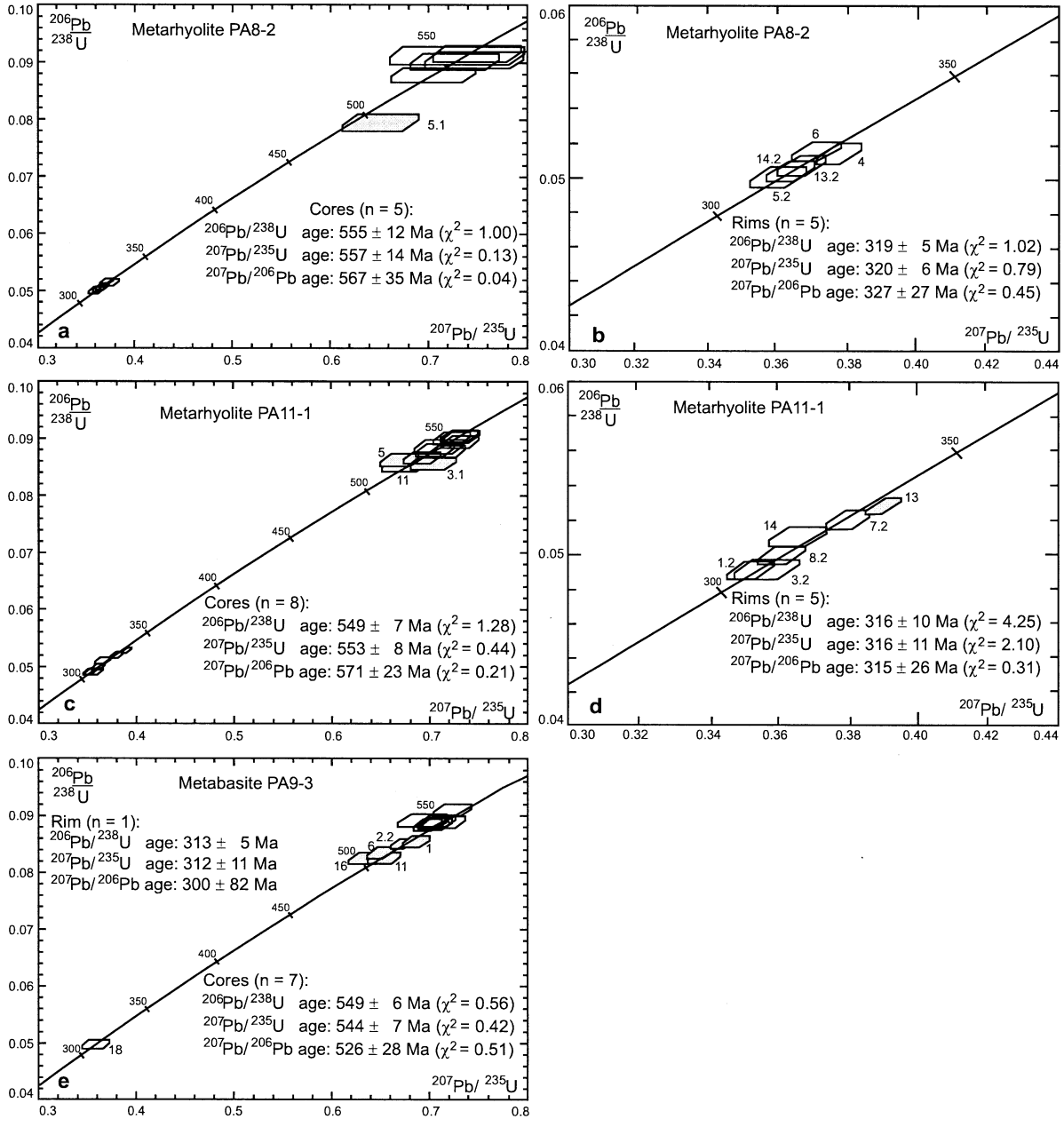

Fig. 4 Concordia diagrams displaying ion-microprobe data for samples from the Passau area (a, c, e); enlarged in right column (b, d). Shaded areas: analyses which were discarded from the calculation of a pooled age. Analytical uncertainties 1σ; all mean ages are at the 95% confidence level

beam completely inside; mixed analyses of outer and inner rims have ages of 314±4 and 316±4 Ma. Pooling of all analyses of inner and outer rims yields a statistically significant mean age of 319±5 Ma (n = 5; χ^2 = 1.02).

Metarhyolite PA11-1 contains a homogeneous population of euhedral, mostly colourless zircons with occasional biotite and fluid inclusions. Zircons show identical, four-part internal structures (Fig. 3b): large, subhedral cores consisting of structureless inner core zones and frequently faded, oscillatory zoned outer core zones are surrounded and in places intruded by non-luminescent, occasionally discontinuous inner rims, which in turn are enclosed by dark, unzoned outer rims, sometimes with strongly faded oscillatory zoning.

The pooled mean age of eight analyses of structureless inner core zones and oscillatory outer core zones is 549±7 Ma (Fig. 4b). Both types of core zone have identical Th/U ratios (0.60–0.78 and 0.62–0.95, respectively), U and Th concentrations. Three analyses were excluded from the calculation of the pooled age: analyses 3.1 and 5 show normal and reverse discordance, respectively; analysis 11 is concordant at 526±7 Ma. Five analyses of inner and outer rims yield a pooled mean age of 316±10 Ma with a high χ^2 of 4.25 indicating excess

scatter. CL imaging reveals that the two youngest ages of 309±3 and 309±4 Ma (spots 1.2, 3.2; Fig. 4b) were determined exclusively on low-CL, outer rims (Fig. 3b), whereas older ages ranging from 314±3 to 326±3 Ma (spots 7.2, 8.2, 14) comprise outer rims as well as non-luminescent inner rims in various proportions due to the small size of the rims. One discordant analysis (spot 13) with an apparent $^{206}Pb/^{238}U$ age of 331±3 Ma is a mixture of a non-luminescent inner rim and a core, and was thus discarded from calculation of the pooled age.

Zircons of *metabasite PA9-3* occur as euhedral crystals, or strongly corroded with pitted surfaces (Fig. 3c). They are predominantly long-prismatic and pink – some transparent, some metamict; smaller individuals are clear and transparent. Rarely, there are opaque inclusions or fluid inclusions. Internal morphology is similar in all individuals: large, euhedral to subhedral cores with medium to low CL dominate the zircon crystals, whereas rims are only very thin. Most cores have a structureless inner zone and an oscillatory outer zone suggesting magmatic formation of both domains. Cores showing homogeneous, often high-CL patches with curved boundaries, truncating existing structures were partly subjected to transgressive recrystallization (Fig. 3c). Rims are typically thin and completely recrystallized with high CL. In places, they intrude into core domains with curved or amoeboid boundaries. Rarely, relic planar growth zoning is preserved in rims. Between core and rim there may be small, non-luminescent domains.

Analyses of structureless inner core zones and oscillatory zoned outer core zones yield similar Th, U and Pb values; Th/U ratios are >1.0, typical for magmatic zircons from mafic rocks (Heaman et al., 1990). The pooled mean age of 549±6 Ma (n =7) is interpreted as the age of magmatic zircon crystallization (Fig. 4c). Five analyses were discarded from the calculation of the pooled mean age: spots 11, 16 and 6 yield ages between 510±6 and 516±5 Ma in domains with recrystallized, partly irregular CL structures; two analyses in partly recrystallized, strongly faded oscillatory zoned and structureless domains have apparent ages of 527±6 and 525±5 Ma (spots 1 and 2.2). Analysis 2.1 is from the same core as 2.2 and yields an apparent age of 548±6 Ma.

With one exception, high-CL rims were too thin to place the ion beam completely on a rim. Analysis of one recrystallized rim, partly unzoned, partly with relic planar zoning, with Th/U = 0.22 (spot 18; Fig. 3c, 4c) yields an apparent age of 313±5 Ma, interpreted to reflect a metamorphic overprint.

Zircons from *metagranitoid HBW1-1* are predominantly euhedral but show some variability in their morphological features. The habit is prismatic; long-prismatic and acicular crystals are strongly dominated by one prism, while short-prismatic individuals have two equally developed prisms. Zircons are mostly pink, sometimes slightly metamict, and often contain inclusions. There are transitions between metamict and transparent crystals. Slightly metamict individuals may be pitted. In contrast to the morphological variability, the internal structures of these zircons, as revealed by CL, are fairly homogeneous (Fig. 3d). Characteristic features are dark, often non-luminescent outer zones with faded or relic oscillatory zoning, and high-CL inner zones, partly recrystallized, partly with faded oscillatory zoning. The euhedral, oscillatory zoning of both the inner and outer zones is continuous throughout the majority of crystals and determines the external shape. This speaks in favour of a continuous growth of the two contrasting zones of these crystals and a common formation. Some zircons show CL evidence for inherited cores; these are often subhedral, in places resorbed. Inherited cores have medium CL intensities, are strongly recrystallized, and often reveal relics of faded oscillatory zoning. An inherited core yields a strongly discordant apparent $^{206}Pb/^{238}U$ age of 1951± 18 Ma (spot 10.2; Fig. 3d). Two younger cores have a reversely and a normally discordant apparent age of 597±6 Ma (spot 8.1; Fig. 5a) and 614±7 Ma (spot 3.1), respectively. 13 analyses of high-CL inner zones and non-luminescent outer zones define a concordant, pooled mean age of 480±6 Ma (Fig. 5a). High-CL inner zones have Th/U ratios of 0.33-0.74 consistent with a partly overprinted, magmatic origin. Dark and non-luminescent outer zones have similar Th contents and higher U and Pb concentrations. Although relatively low, Th/U ratios of 0.10–0.14 are above typical metamorphic values (Rubatto et al., 1999; Schaltegger et al., 1999; Williams et al., 1996), and argue against recrystallization by external fluids. Despite different CL intensities, the apparent ages from both zones are identical within error, thus suggesting a common formation during the same magmatic cycle. A non-luminescent rim (spot 8.2) with extremely high U (5391 ppm) and Pb (310 ppm) yields a reversely discordant (111% concordance) $^{207}Pb/^{206}Pb$ age of 487±6 Ma, similar to the pooled age. Analysis 10.1 yielding a concordant age of 433±4 Ma and the strongly discordant analysis 2.2 show transgressively recrystallized CL structures, and have been omitted from calculation of the pooled age.

Metagranitoid HBW31-2 contains zircons which are predominantly euhedral, colourless and inclusion-poor to inclusion-free. Their habit is short- to long-prismatic; rounded grains, slightly corroded crystals and growth inhibitions are rare features. CL imaging reveals complex, internal structures (Fig. 3f), similar to sample HBW1-1: zircons with rounded cores and rims on the one hand, and crystals with continuous growth on the other hand. Continuously grown zircons often have oscillatory zoned inner zones with high CL and dark or non-luminescent outer zones with relic oscillatory zoning. Zircons with rounded cores usually have a strongly recrystallized, high-CL inner rim and a thin dark to non-luminescent outer rim, identical to the inner and outer zones of continuously grown zircons. Rounded cores show oscillatory zoning; rarely, they are completely recrystallized (spots 10, 22; Fig. 3f). Zircon cores are sometimes resorbed by non-luminescent domains.

Inherited cores appear as two different types (Fig. 5e, f): two analyses of cores with faded oscillatory zoning and

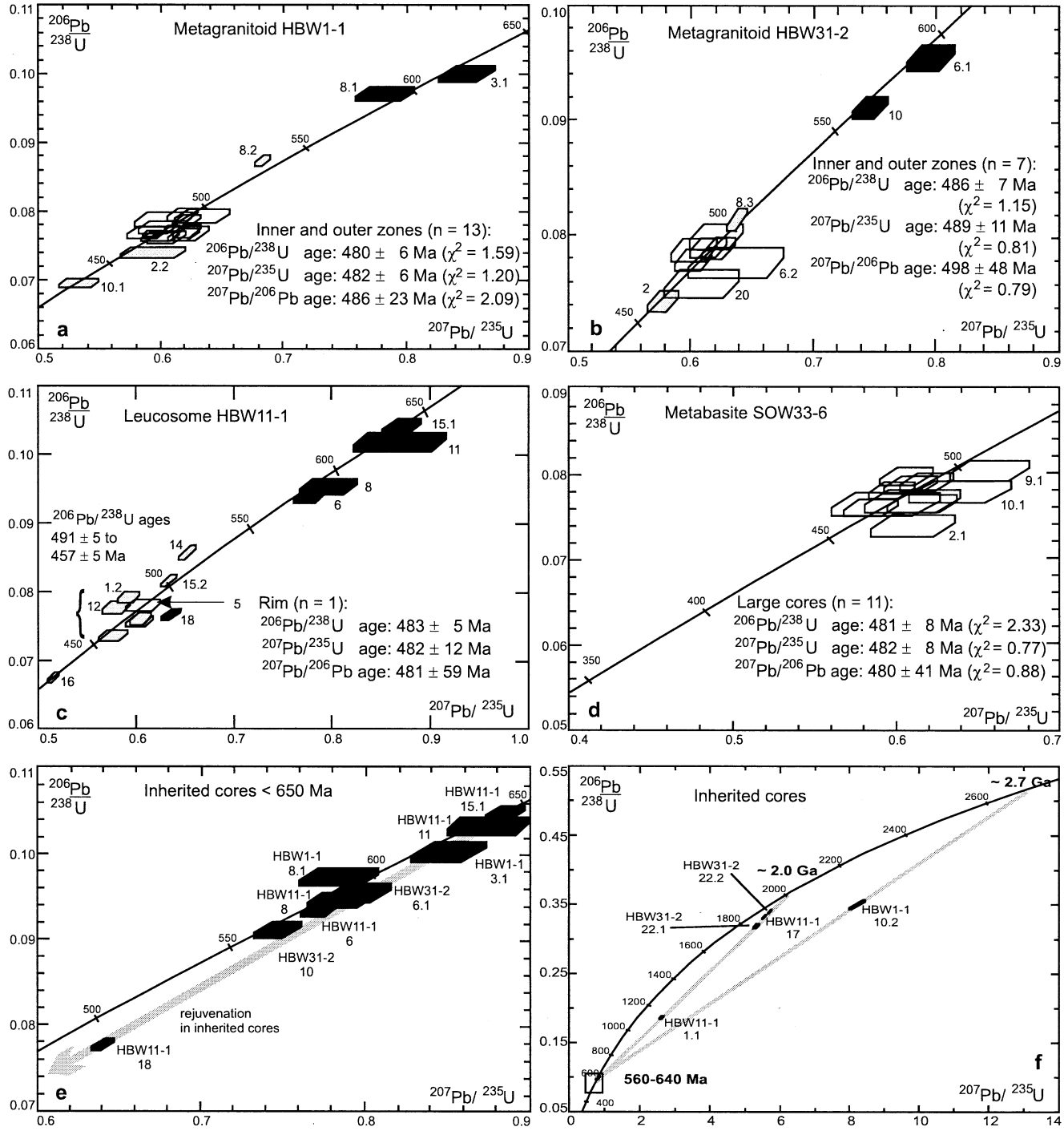

Fig. 5 Concordia diagrams displaying ion-microprobe data for samples from the Hinterer Bayerischer Wald (a-c, e, f) and the southern Oberpfälzer Wald (d). Black areas: analyses of inherited cores. Shaded areas: analyses which were discarded from the calculation of a pooled age. Inherited cores of samples HBW1-1, HBW31-2 and HBW11-1 are plotted together in diagrams e and f. Analytical uncertainties 1σ; all mean ages are at the 95% confidence level

Th/U ratios slightly below magmatic values (0.36–0.45) yield slightly discordant apparent $^{206}Pb/^{238}U$ ages of 562±6 Ma (spot 10) and 587±7 Ma (spot 6.1). In contrast, two cores with completely recrystallized CL structures have strongly discordant $^{206}Pb/^{238}U$ ages of 1790±18 Ma (spot 22.1) and 1890±17 Ma (spot 22.2); $^{207}Pb/^{206}Pb$ ages are 1982±21 and 1993±7 Ma. Both cores are incorporated in the same crystal (Fig. 3f): a rounded, outer core with extremely high CL and relic oscillatory zoning contains a rounded, non-luminescent, inner core with high U content (1495 ppm). Seven analyses of rims with recrystallized or faded oscillatory zoning define a pooled mean age of

486±7 Ma (Fig. 5b). Th/U ratios between 0.17 and 0.74 are well above typical metamorphic values and indicate magmatic zircons as well as progressively overprinted, originally magmatic zircons. Two analyses have been excluded from calculation of the pooled age: one rim (spot 2) with an intermediate Th/U ratio (0.3) and an apparent age of 462±5 Ma, and a non-luminescent, outer rim (spot 8.3) with high U (1922 ppm), a very low Th/U ratio (0.05) and an apparent $^{206}Pb/^{238}U$ age of 503±5 Ma. The $^{207}Pb/^{206}Pb$ age of the high U analysis is 498±13 Ma.

Zircons of *leucosome HBW11-1* range from strongly corroded, subhedral to euhedral, short- to long-prismatic crystals. Most zircons show partial to complete metamictization in transmitted light. The high proportion of metamict zircons clearly separates this sample from leucocratic metamagmatite samples described above. More or less clear zircons are often smaller, short-prismatic, containing inclusions. Internal structures of the investigated zircons show a variety of features suggesting considerable overprint of originally magmatic/anatectic zircons and inherited zircons (Fig. 3). Generally, zircons have one or two rims with rounded cores or concordant inner zones. Thin outer rims are homogeneously recrystallized with medium to suppressed CL, probably being the result of fluid-related, late-stage recrystallization. In all other domains relic oscillatory zoning or planar structures pointing to a magmatic origin may be present. Nonetheless, most zircons are largely recrystallized, sometimes patchy, sometimes with convoluted (Fig. 3e, grain 10) or curvilinear structures suggesting migration of recrystallization fronts (Pidgeon, 1992; Vavra et al., 1996; Williams et al., 1996).

As can be expected from the diversity of internal structures, the geochronological data is complex. Similar to samples HBW1-1 and HBW31-2 there are two types of zircon cores (Fig. 5e, f). Two strongly recrystallized, inherited cores have highly discordant, apparent $^{206}Pb/^{238}U$ ages of 1112±11 Ma (spot 1.1; Fig. 5f) and 1856±17 Ma (spot 17); $^{207}Pb/^{206}Pb$ ages are 1614±15 and 1978±7 Ma, respectively. The second type of inherited cores also has recrystallized CL structures but relic oscillatory zoning is still preserved. These core ages scatter around a line: the oldest age is concordant at 637±7 Ma (spot 15.1), younger core ages get increasingly discordant. The youngest, most discordant core (spot 18; Fig. 5e) yields a $^{206}Pb/^{238}U$ age of 476±5 Ma; its $^{207}Pb/^{206}Pb$ age of 610±13 Ma is similar to the oldest, concordant core age.

Six analyses from rims, inner and outer zones showing evidence for recrystallization as well as relic oscillatory zoning yield concordant to slightly discordant, apparent ages ranging from 491±5 to 457±5 Ma (Fig.5c); the pooled $^{206}Pb/^{238}U$ age of 474±13 Ma shows large excess scatter with $\chi^2 = 4.92$ and is statistically not significant. The variety of internal structures (faded oscillatory zoning, transgressive and convoluted structures), intermediate Th/U ratios (0.02 to 0.33) and deduced processes (magmatic/anatectic formation, annealing, recrystallization) as well as the spread of data argue against combining these ages to a pooled age. Some analyses of non-luminescent domains show extremely high U contents (5517–6833 ppm); one analysis yields a $^{207}Pb/^{206}Pb$ age of 431±7 Ma (spot 16; Fig. 5c); the other two analyses (spots 14, 15.2) show reverse discordance with $^{207}Pb/^{206}Pb$ ages of 456±6 and 469±6Ma.

Metabasite SOW33-6 from the Oberviechtach area contains a single population of clear, strongly corroded, long- and short-prismatic zircons. Internal morphology as revealed by CL imaging is homogeneous throughout the population (Fig. 3g): large cores with faded oscillatory zoning are overgrown and partly resorbed by thin high-CL overgrowths; patchy, medium-CL, transgressive recrystallization is also wide-spread. Cores are usually not rounded but subhedral to euhedral. Th/U ratios ranging from 0.18 to 0.33 are well below ratios typical for magmatic zircons from mafic rocks (Th/U >1.0; Heaman et al., 1990). Pb contents are very low (5–24 ppm) in the analyzed zircons.

11 core analyses yield a pooled age of 481±8 Ma (Fig. 5d) with $\chi^2 = 2.33$ implying excess scatter.

Nd isotope data

Sm-Nd isotope data for 13 samples of metarhyolites, metagranitoids, metabasites and leucosomes are listed in Table 3. Initial ϵ_{Nd} values ($\epsilon_{Nd(t)}$) were calculated for the corresponding magmatic U-Pb ages (PA8-2, PA11-1, PA9-3, HBW1-1, HBW31-2, this study; KG2-2, SOW9-1, Mielke et al., 1996) or estimated by comparison with dated samples on the basis of geochemical, petrographic and regional geologic criteria (HBW7-1, SOW3-2, SOW30-2, HBW12-3, HBW14-1, SOW13-1).

The analyzed leucocratic gneiss samples show a large variation in $\epsilon_{Nd(t)}$ values, -0.50 to -6.27, indicating highly variable proportions of juvenile and old, recycled continental crust. $\epsilon_{Nd(t)}$ values are well above typical values of metasediments exposed in the western Bohemian Massif (Ihlenfeld et al., 1998; Liew and Hofmann, 1988) except for metarhyolite sample KG2-2. For samples with typical crustal $^{147}Sm/^{144}Nd$ ratios around 0.12 (Liew and Hofmann, 1988) the $\epsilon_{Nd(t)}$ values correspond to Nd model ages (T_{DM}) of 1.18–1.47 Ga. Five samples (leucosomes; metarhyolites SOW3–2, KG2–2) have unusually high $^{147}Sm/^{144}Nd$ ratios >0.14, suggesting Sm/Nd fractionation during magma genesis and resulting in unrealistically old Nd model ages of 1.85–3.85 Ga. Therefore, two-stage Nd model ages ($T_{DM\ 2}$) were calculated for these samples according to Liew and Hofmann (1988), ranging from 1.37 to 1.65 Ga. In contrast to Mesoproterozoic Nd model ages (1.18–1.65 Ga), evidence from U-Pb dating of inherited zircons only documents Neoproterozoic (560–640 Ma) and Palaeoproterozoic-Archaean (2.0–2.7 Ga) components. Thus, the Nd model ages represent mixing ages (Arndt and Goldstein, 1987) of Neoproterozoic and Palaeoproterozoic-Archaean crustal portions.

Relatively high, negative $\epsilon_{Nd(t)}$ values (-3.01 and -1.66) for two ~ 550 Ma PA metarhyolites (PA8-2, PA11-1) point to small proportions of recycled, older crust, con-

Table 3 Sm-Nd isotope data. Age determined by independent U-Pb dating (PA8–2, PA9–3, PA11–1, HBW1–1, HBW31–2; this study; SOW9–1, KG2–2; Mielke et al., 1996) or estimated by comparison with geochemcally and petrographically similar samples of known age (HBW7–1, SOW3–2, SOW30–2, HBW12–3, HBW14–1, SOW13–1). Nd model ages T_{DM} and two-stage Nd model ages $T_{DM(2)}$ for samples with $^{147}Sm/^{144}Nd > 0.14$ are calculated according to Liew and Hofmann (1988) for leucocratic gneisses. MR: metarhyolite; MG: metagranitoid; MB: metabasite; Leu: leucosome

Sample	Group	Age t	Sm	Nd	$^{147}Sm/^{144}Nd$	$^{143}Nd/^{144}Nd$	$\pm 2\sigma_M$	$\epsilon_{Nd(0)}$	$\epsilon_{Nd(t)}$	T_{DM}	$T_{DM(2)}$
		[Ma]	[ppm]	[ppm]						[Ga]	[Ga]
			±1%	±1%	±0.5%	±0.005%					
PA8–2	MR	555	11.91	59.24	0.1215	0.512211	6	−8.33	−3.01	1.47	–
PA9–3	MB	549	3.04	11.90	0.1546	0.512549	8	−1.74	+1.22	–	–
PA11–1	MR	549	8.05	44.88	0.1085	0.512238	8	−7.80	−1.66	1.26	–
HBW1–1	MG	480	4.38	22.54	0.1174	0.512363	9	−5.36	−0.50	1.18	–
HBW7–1	MG	485	5.70	29.78	0.1157	0.512159	9	−9.34	−4.37	1.46	–
HBW31–2	MG	486	5.82	28.76	0.1224	0.512274	10	−7.10	−2.49	1.38	–
SOW3–2	MR	475	2.60	10.16	0.1549	0.512371	9	−5.21	−2.68	(1.85)	1.37
SOW9–1	MR	475	2.46	11.63	0.1277	0.512326	10	−6.08	−1.89	1.37	–
SOW30–2	MB	480	2.94	7.78	0.2287	0.513140	13	+9.80	+7.84	–	–
KG2–2	MR	475	7.55	31.65	0.1443	0.512154	12	−9.44	−6.27	(2.03)	1.65
HBW12–3	Leu	475	1.10	4.17	0.1592	0.512325	8	−6.10	−3.80	(2.09)	1.46
HBW14–1	Leu	475	1.13	3.58	0.1899	0.512407	11	−4.50	−4.08	(3.85)	1.48
SOW13–1	Leu	475	0.23	0.92	0.1524	0.512225	14	−8.06	−5.34	(2.11)	1.58

sistent with the lack of inherited zircons in these samples. Associated with these metarhyolites is a metabasite (PA9-3); a slightly positive $\epsilon_{Nd(t)}$ value of +1.22 indicates an enriched mantle source (mantle plume, intracontinental rifting or subcontinental lithosphere) or crustal contamination (Pin and Paquette, 1997).

A similar range of high, negative $\epsilon_{Nd(t)}$ values (-2.68 to -1.89) is found in ~ 475 Ma SOW metarhyolites, also consistent with small proportions of old recycled crust. One metabasite from the vicinity (SOW30-2) is derived from a depleted mantle reservoir as evidenced by a high, positive $\epsilon_{Nd(t)}$ value (+7.87), consistent with its geochemical normal MORB signature.

The lowest $\epsilon_{Nd(t)}$ value of -6.27 occurs in sample KG2-2, a ~ 475 Ma KG metarhyolite, implying melting of a considerable proportion of old crustal material.

HBW metagranitoids of Lower Ordovician age (~ 485 Ma) show a large variation of $\epsilon_{Nd(t)}$ values, ranging from -0.50 to -4.37, indicative of strongly varying proportions of juvenile (?volcanic arc) and old crustal material.

Leucosomes from the Bodenmais – Waldmünchen area are characterized by fairly uniform, low $\epsilon_{Nd(t)}$ values between -3.82 and -5.37. Although similar in crystallization age (~ 485 Ma) and of close geographical relationship to HBW metagranitoids and SOW metarhyolites, the leucosomes analyzed seem to contain higher proportions of recycled continental crustal material, consistent with their crustal, anatectic origin. Nonetheless, $\epsilon_{Nd(t)}$ values are slightly above typical values of metasediments exposed in the western Bohemian Massif (Ihlenfeld et al., 1998; Liew and Hofmann, 1988).

Interpretation and Discussion

Precambrian Basement

Evidence of the Precambrian basement in the Bayerischer Wald comes from inherited zircons and from Nd isotope data. Mechanically rounded and/or chemically resorbed, inherited zircon cores were found in metagranitoid and leucosome samples HBW1-1, HBW31-2 and HBW11-1 only (Fig. 3; Fig. 5e, f). They consist of recrystallized, discordant, originally Palaeoproterozoic-Archaean zircons (group I), and concordant to discordant, Neoproterozoic zircons with faded oscillatory zoning (group II) indicating progressively overprinted, magmatic zircons. Apparent $^{206}Pb/^{238}U$ ages of most group-II zircons range from 562±6 to 637±7 Ma; one core with strongly recrystallized CL structures (HBW11–1, spot 18) has a younger, discordant age. Group-II zircons roughly align on a regression line with an upper intercept age of 623±56 Ma (MSWD = 0.32) which is comparable to the concordant age of the oldest group-II zircon (637±7 Ma). This concordant age is taken as a tentative estimate for the magmatic formation of these zircon cores. Discordant group-I zircons point to upper intercept ages of ~ 2.0 Ga and ~ 2.7 Ga (Fig. 5f). From the pattern of ages and the contrasting internal morphology of group-I and group-II zircons it is assumed that Neoproterozoic group-II zircons crystallized in a ~ 640 Ma magmatic event as part of the wide-spread subduction-related, Cadomian magmatism in Gondwana-derived terranes (Linnemann et al., 2000; Nance et al., 1991), and that recrystallized, originally ~ 2.0 and ~ 2.7 Ga old group-I zircons suffered Pb loss while being incorporated into Cadomian magmas at ~ 640 Ma.

The ~ 2.0 and ~ 2.7 Ga old, inherited zircons fit well into the range of inherited and detrital zircon ages known from the Bayerischer Wald and southern Bohemia of 1.7–

2.0, 2.4, 2.6–2.7 and 3.8 Ga (Gebauer et al., 1989; Grauert et al., 1973; Kröner et al., 1988; Propach et al., 2000; Teufel, 1988); they are also consistent with direct evidence of Palaeoproterozoic basement in the Bohemian Massif provided by 2104–2048 Ma old orthogneisses (Wendt et al., 1993).

Possible source rocks for the inherited Palaeoproterozoic-Archaean zircons are located at the northern Gondwana margin (compilations in Nance and Murphy, 1996 and Söllner et al.,1997). Lack of Mesoproterozoic zircon ages suggests affinities to the West African craton (Fernández-Suárez et al., 2002; Nance and Murphy, 1996). The range of $\epsilon_{Nd(t)}$ values (-0.5 to -6.27) is also found in the Armorican terrane assemblage (Nance and Murphy, 1996). Corresponding Mesoproterozoic Nd model ages of 1.18 to 1.65 Ga are interpreted to reflect mixing of Palaeoproterozoic-Archaean and Neoproterozoic components. Neoproterozoic, ~ 640 Ma zircons are seen as evidence for the wide-spread, subduction-related Cadomian magmatism in terranes derived from the northern Gondwana margin (Nance et al., 1991).

Upper Vendian magmatism (~ 550 Ma)

In the south-western part of the Bayerischer Wald – in the Passau area – Upper Vendian acid and basic magmatism is documented by zircon ages of 555±12, 549±7 and 549±6 Ma from metarhyolites and one metabasite (PA8-2, PA11-1, PA9-3). Old, inherited cores were not detected in zircons of these samples. Zircons of metarhyolite PA11-1 and metabasite PA9-3 have identical ages and similar internal morphologies displaying primary, magmatic structures (oscillatory zoning, structureless inner zones) and minor secondary structures (fading, recrystallization). Individual ages of both primary and secondary domains are identical within error and show little spread. The pooled ages represent magmatic formation ages. Another metarhyolite (PA8-2) yields a pooled age of 555±12 Ma (without excess scatter) defined by high-CL zircon cores. The pooled age is interpreted as a magmatic formation age, analogous to samples PA11-1 and PA9-3. However, the nature and timing of the overprinting that lead to transformation to high-CL zircon is not clear. Relatively high Th/U ratios argue against recrystallization of hypothetical, pre-existing zircon by external (metamorphic or hydrothermal) fluids with complete isotopic resetting of the U-Pb system during a 550 Ma event; rejection of this hypothesis is substantiated by the lack of pre-550 Ma zircons in the other two samples from the same area. This phenomenon is possibly related to the high proportion of cm-sized leucosomes in sample PA8-2, indicating a more intense, high-grade overprint than in the other two PA samples. This would imply that annealing/recrystallization did not reset the U-Pb system and therefore preserved the same age information as non-recrystallized zircon from the other two samples. Survival of magmatic zircon and preservation of original crystallization age information in rocks that experienced an ultra high temperature overprint is shown by Möller et al. (2002), implying that resetting of zircon by diffusion during high-grade metamorphism is negligible.

Two PA samples have zircons with apparent $^{206}Pb/^{238}U$ ages slightly younger than ca. 550 Ma. Concordant to reversely discordant ages between 510±6 and 516±5 Ma were determined in domains with recrystallized, partly irregular CL structures (PA9-3); due to CL evidence these ages are interpreted to reflect rejuvenation by fluid- or partial-melt-driven recrystallization. Three analyses from sample PA9-3 and PA11-1 cluster concordantly to slightly discordantly at 525±5 to 527±6 Ma. Concordance of data points may indicate zircon growth at 525 Ma; similar ages are known from the Teplá-Barrandian from intrusions emplaced into transtensive shear zones (Dörr et al., 2002) and from the Silvretta area in the Alps (Schaltegger et al., 1997) pointing to early Cambrian magmatism there. CL imaging, however, reveals strongly faded oscillatory zoned and structureless domains, partly with recrystallized structures pointing to overprinting of magmatic zircon. Additional age and CL data is required for further evaluation of the significance of this 525 Ma age cluster.

Geochemical data of Upper Vendian PA metarhyolites suggest continental and/or subduction-related influences. Relatively high, negative $\epsilon_{Nd(t)}$ values (-3.01 to -1.66) point to magma sources with variable but small proportions of old, continental crustal material, consistent with the lack of inherited zircons. An associated metabasite showing an enriched MORB signature and subduction influence (Teipel, 2003) is presumably derived from a subcontinental lithospheric mantle source ($\epsilon_{Nd(t)}$ +1.22). Geochemical signatures of the PA metarhyolites and the metabasite suggest a position at an active continental margin, probably with back arc development, for the Upper Vendian magmatism.

Lower Ordovician magmatism (~ 485-475 Ma)

In contrast to the south-western part, the Hinterer Bayerischer Wald, the southern Oberpfälzer Wald and the Künisches Gebirge – in the north-eastern parts of the Bayerischer Wald – are characterized by Lower Ordovician magmatism.

HBW metagranitoids yield pooled mean ages of 480±6 Ma and 486±7 Ma (HBW1-1, HBW31-2). Both mean ages are identical within error and are interpreted as magmatic crystallization ages. The slightly younger mean age of sample HBW1-1 might to some extent be biased by secondary processes as indicated by minor excess scatter (χ^2 = 1.59), faded magmatic CL structures and intermediate to high Th/U ratios (0.1–0.74) indicating magmatic zircons as well as variably overprinted, originally magmatic zircons. High U zircons yield $^{207}Pb/^{206}Pb$ ages of 487±6 Ma (HBW1-1, spot 8.2) and 498±13 Ma (HBW31-2, spot 8.3). Further age constraints for Lower Ordovician acid magmatism have been reported by Mielke et al.

(1996) with SHRIMP ages of ~ 475 Ma from the SOW and KG.

Leucosome sample HBW11-1 displays a more complex zircon evolution with well-rounded, sometimes eccentric cores, faded oscillatory zoning, transgressive and convoluted structures, and low to intermediate Th/U ratios (0.02 to 0.33). This is consistent with its migmatitic origin, suggesting anatectic zircon formation and related overprinting in the period 491±5 to 457±5 Ma. The concordant, individual age of 483±5 Ma of a faded oscillatory zoned rim (spot 5; Fig. 3e) may be seen as the best estimate for the magmatic/anatectic event. Two reversely discordant analyses with high U yield $^{207}Pb/^{206}Pb$ ages of 456±6 and 469±6 Ma (spots 14, 15.2; discussed below).

In the southern Oberpfälzer Wald, a probably tectonically-emplaced, retrogressed eclogitic amphibolite (O'Brien, 1989b; O'Brien et al., 1997) yields a pooled age of 481±8 Ma (SOW33-6). Excess scatter of age data, faded magmatic internal structures, patchy recrystallization structures and intermediate Th/U ratios are evidence for variable overprinting of originally magmatic zircons. The pooled mean age is interpreted as a minimum age for magmatic crystallization. CL structures of thin overgrowths with high CL and often transgressive boundaries are consistent with their formation under amphibolite- or eclogite-facies conditions (Rubatto, 2002; Schaltegger et al., 1999). These overgrowths have not been analyzed due to their small size. So far, Ordovician metabasite protolith ages have not been reported for the Moldanubian of the Bayerischer Wald. Lower Ordovician basic magmatism is known from the Zone of Erbendorf-Vohenstrauß (ZEV) and the Mariánské Lázně Complex (Teplá-Barrandian) with U-Pb zircon ages of 483±8 to 496±8 Ma (Bowes and Aftalion, 1991; von Quadt, 1997).

Lower Ordovician leucocratic metamagmatites from the Hinterer Bayerischer Wald, the southern Oberpfälzer Wald and the Künisches Gebirge show geochemical characteristics indicative of continental crust and/or subduction. Calc-alkaline HBW metagranitoids with inherited Neoproterozoic and Palaeoproterozoic-Archaean zircons are derived from mixed magma sources with old, recycled (Gondwana crust) and juvenile (Cadomian volcanic arc) material, as evidenced by $\epsilon_{Nd(t)}$ values of -0.50 to -4.37. SOW metarhyolites with relatively high $\epsilon_{Nd(t)}$ values (-2.68 to -1.89) are presumably derived from a more juvenile, subduction-related precursor. A low $\epsilon_{Nd(t)}$ value (–6.27) of a KG metarhyolite indicates a high amount of old continental crustal material in the magma source. Associated calc-alkaline, andesitic metabasites from the Künisches Gebirge are consistent with an active continental margin geotectonic setting (Teipel, 2003). SOW metabasic rocks representing HP relics ("Winklarn series") have MORB-type geochemistry (O'Brien, 1989a) as exemplified by normal MORB geochemical and Nd signatures ($\epsilon_{Nd(t)}$ = +7.87) of sample SOW30-2. As these Lower Ordovician metabasic rocks are probably tectonically emplaced, their geotectonic position is not directly linked to SOW metarhyolites with subduction characteristics. Lower to Middle Ordovician anatexis as documented by SHRIMP ages between 491 and 459 Ma of leucosome HBW11-1 probably took place in lower levels of thickened crust; today's spatial proximity to metarhyolites and metagranitoids can be explained by crustal imbrication during subsequent collisional events. Ordovician anatexis has been proposed before on the basis of Rb-Sr whole-rock ages ranging from 490–470 Ma (Grauert et al., 1974; Köhler et al., 1989) and U-Pb zircon and monazite data from migmatitic paragneisses at ~ 460 Ma (Gebauer et al., 1989; Teufel, 1988).

A geotectonic position in a convergent setting, probably at an active continental margin, is assumed in the north-eastern parts of the Bayerischer Wald for the Lower Ordovician. Some variation in the proportions of juvenile versus old, continental material may be deduced from minor geochemical and Nd isotopic heterogeneity. Geochemical or isotopic proof of rift-related magmatism was not found. Coeval normal MORB metabasites of the "Winklarn series" are interpreted as equivalents of ZEV and Mariánské Lázně Complex metabasites (O'Brien, 1989b; O'Brien et al., 1997). They may represent relics of (?subducted) ocean floor possibly neighbouring a Lower Ordovician continental margin.

Zircon evidence for metamorphic overprint

Zircons of metamagmatites from the south-western Bayerischer Wald (PA) show evidence for metamorphic zircon growth. Pooled mean ages of recrystallized rims of 319±5 and 316±10 Ma (metarhyolites PA8-2, PA11-1) and a single rim age of 313±5 Ma (metabasite PA9-3) confirm Variscan metamorphism in the Carboniferous. Zircons of the metarhyolites are characterized by two separate rims: Inner rims with low to completely suppressed CL show features typical for an anatectic origin (Th/U ratios <0.01, sometimes resorbing the core; Williams, 2001); they are particularly well developed in sample PA8-2 which has a high proportion of cm-sized leucosomes. Outer rims are usually unzoned with low Th/U ratios, or rarely have faded oscillatory zoning. These outer rims resemble zircons recrystallized by fluids under amphibolite- or eclogite-facies conditions (Rubatto, 2002; Rubatto et al., 1999; Schaltegger et al., 1999). Relating this CL information to the age data, three analyses unequivocally in outer rims (PA11-1: spots 1.2, 3.2; PA9-3: spot 18) yield ages between 309±4 and 313±5Ma; most other analyzed spots represent mixing between inner and outer rims in varying proportions with ages ranging from 314±4 to 326±3Ma. Although the ages partly overlap in error, by taking into account the CL information it may be suspected from these few data that two metamorphic stages are represented: outer rims document a younger, probably fluid-related stage of metamorphism around 309–313 Ma identical to Ar-Ar biotite ages (309–313 Ma, northern Bayerischer Wald; Kalt et al., 2000), whereas non-luminescent inner rims represent an older, most likely anatectic stage some time between 314 and

326 Ma in accordance with U-Pb monazite and zircon data of 316–326 Ma dating LPHT peak conditions (Grauert et al., 1974; Kalt et al., 2000; Propach et al., 2000; Teufel, 1988).

In contrast, no Variscan, metamorphic zircon growth has been directly dated in the investigated zircons from the north-eastern Bayerischer Wald (HBW, SOW) in this study. CL imaging reveals only very small high-CL patches and overgrowths in some of the investigated zircons which might be interpreted as fluid-related (metamorphic?) overgrowths; these were too small to be analyzed. However, Variscan U-Pb ages of zircon tips of 323 to 326 Ma have been reported from this area dating LPHT peak conditions with melt formation (Kalt et al., 2000).

Two analyses from HBW samples HB1-1 (spot 10.1) and HBW 11-1 (spot 16) yield concordant $^{206}Pb/^{238}U$ ages of 433±4 and 420±4 Ma; in the latter case the $^{207}Pb/^{206}Pb$ age of 431±7 Ma is regarded as more significant due to high U content. These ages coincide with Upper Silurian HP metamorphism at 424±13 Ma in the SOW (Sm-Nd mineral isochrone; von Quadt and Gebauer, 1993). It is concluded that the HBW area was affected by metamorphism in the Upper Silurian at ~ 430 Ma.

Samples HBW31-2 and HBW11-1 show two $^{206}Pb/^{238}U$ ages at 462±6 (concordant; spot 2) and 457±6 Ma (slightly discordant; spot10); furthermore, two reversely discordant analyses with high U of sample HBW11-1 yield $^{207}Pb/^{206}Pb$ ages of 456±6 and 469±6 Ma (spots 14, 15.2). As this clustering of ages is not well constrained, its significance is hard to address. In the case of leucosome sample HBW11-1, spot 10, CL information of convolute internal structures suggests overprinting at ~ 460 Ma, coeval to zircon and monazite data from migmatitic paragneisses, interpreted as metamorphic/anatectic ages (Gebauer et al., 1989; Teufel, 1988).

The "Bayerischer Wald" in the context of Gondwana-derived terranes – a tentative palaeogeographic model

Geochronological, geochemical and isotopic results from leucocratic metamagmatites and metabasites from the Bayerischer Wald for the first time allow a tentative reconstruction of the palaeogeographic position of the "Bayerischer Wald" in Upper Vendian and Lower Ordovician times:

Nd isotope data and Palaeoproterozoic-Archaean, inherited zircon cores, consistent with data from other Variscan basement domains in central Europe, suggest an original position of the "Bayerischer Wald" at the northern margin of Gondwana, most likely in the vicinity of the West African craton. Neoproterozoic, inherited zircon cores at ~ 640 Ma (progressively rejuvenated to ~ 560 Ma) are evidence of components of the wide-spread subduction-related, Cadomian magmatism in Gondwana-derived terranes (Linnemann et al., 2000; Nance et al., 1991) inherited in Lower Ordovician metagranitoids. Similar magmatic ages are known from the two large, neighbouring units, the Saxothuringian (Linnemann et al., 2000) and the Teplá-Barrandian (Dörr et al., 2002).

For Upper Vendian (~ 550 Ma) acid and basic magmatism in the south-western part of the Bayerischer Wald an active continental margin setting with ensialic back arc development is inferred; the observed lack of Neoproterozoic or older, inherited zircons may be due to either complete dissolution of pre-existing zircons or derivation from more juvenile magma sources without pre-existing zircons. Corresponding ages and setting have been reported from the Habach terrane (Tauern window, Alps), a terrane of northern-Gondwana affinity, where 551±9 and 547±27 Ma old, subduction-related, basic to intermediate metamagmatites are interpreted as evidence for an ensialic back arc evolution (Eichhorn et al., 1999, 2001). Therefore, a close spatial relationship between the "Bayerischer Wald" and the Habach terrane (proto-Alps) is assumed. Coeval, high-grade metamorphic conditions attributed to microcontinent-collision at the Gondwana margin are evidenced in the Teplá-Barrandian by K-Ar hornblende and U-Pb monazite ages of 551–540 Ma (Bues et al., 2002; Zulauf et al., 1999); collision-related granitoids intruded ~ 540–530 Ma (Dörr et al., 2002; Linnemann et al., 2000). Further U-Pb zircon ages between 520 and 525 Ma mark active continental margin magmatism, probably with back arc development in the Alps (Silvretta, Austroalpine domain; Schaltegger et al., 1997), and transtension-related magmatism in the Teplá-Barrandian (Dörr et al., 2002; Zulauf et al., 1997). These age data reflect the diachronous evolution of subduction-related, Cadomian magmatism in Gondwana-derived terranes (Nance and Murphy, 1996). Proposed strike-slip models involve oblique subduction, ridge-trench collision, pull-apart basins and large-scale transform faults, thus creating different scenarios along the northern Gondwana margin (including e.g. Avalonia and the ATA) in the course of time (Fernández-Suárez et al., 2002; Murphy et al., 2000; Nance et al., 2002).

Lower Ordovician acid and minor basic/andesitic magmatism (~ 485–475 Ma) in the "Bayerischer Wald" suggests essentially convergent settings, probably at an active continental margin, possibly collisional in places. A coeval, convergent setting (island arc – continent collision) is also proposed for the Habach terrane (proto-Alps) at ~ 480 Ma (Eichhorn et al., 2001). In contrast, extensional settings, coeval to rift-related magmatism in Avalonia at ~ 485 Ma (van Staal et al., 1998), are known from most other Variscan massifs in central Europe: in the Saxothuringian at 510–500 Ma and at ~ 480 Ma (Kemnitz et al., 2002; Kröner and Willner, 1998; Linnemann et al., 2000; Mingram, 1998; Schätz et al., 2002), in the French Massif Central at ~ 480 Ma (Pin and Lancelot, 1982; Pin and Marini, 1993), in the ZEV at ~ 495–480 Ma (Söllner et al., 1997; von Quadt, 1997); back arc or continental rifting is assumed at 490–470 Ma in the Schwarzwald (Chen et al., 2003); intracontinental rifting

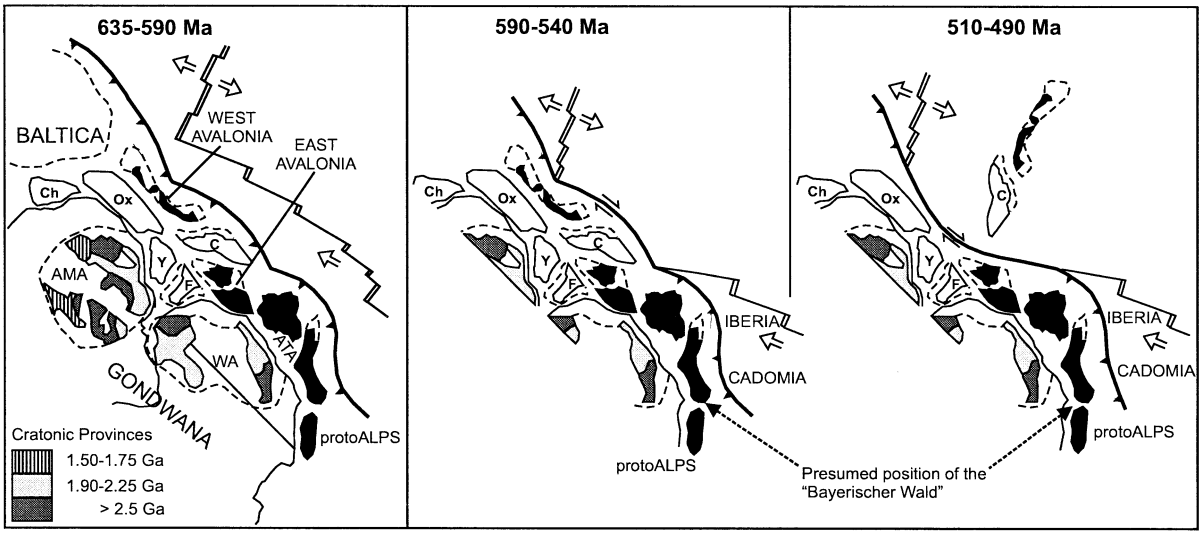

Fig. 6 Palaeogeographic reconstruction of peri-Gondwana terranes relative to Gondwana (modified after Nance et al., 2002); the position of the proto-Alps is modified after Schätz et al. (2002), Tait et al. (2000) and von Raumer et al. (2002). AMA: Amazonian craton; WA: Westafrican craton; ATA: Amorican terrane assemblage, comprising Iberia and Cadomia. Gondwana-derived terranes marked in black are mentioned in the text (Ch: Chortis Block; Ox: Oaxaquia; Y: Yucatan Block; F: Florida; C: Carolina). 635–590 Ma: Neoproterozoic subduction at the northern Gondwana margin. 590–540 Ma: Upper Vendian ridge-trench collision in the West Avalonia area with diachronous termination of subduction and generation of large-scale transform fault. Prolonged subduction in the vicinity of the ATA (Iberia, Cadomia) and probably the proto-Alps. 510–490 Ma: Early Palaeozoic continuation of the diachronous evolution with rifting of West Avalonia and persistent convergence/subduction outboard of the ATA and the proto-Alps. The presumed position of the "Bayerischer Wald" between Cadomia and the proto-Alps is indicated

is suggested in the Northern Greywacke Zone (Alps) at ~ 475 Ma (Loth et al., 2001; Schauder, 2002).

Successive rifting and drifting of Gondwana-derived terranes started in the Lower Ordovician (Tait et al., 1997) and probably occurred diachronously – starting in the "western" terranes (West- and East-Avalonia) – due to ridge-trench-collision in the West-Avalonia area (Fernández-Suárez et al., 2002; Nance et al., 2002). Assuming a diachronous evolution at the northern margin of Gondwana, there should be convergence and/or subduction in the "eastern" parts of the chain of Gondwana-derived terranes, whereas further to the "west" rifting already took place or started to take place (Fig. 6). Consequently, the "Bayerischer Wald" is tentatively placed at an"eastern" position in the chain of Gondwana-derived terranes in the Lower Ordovician. The presumed, Lower Ordovician position of the "Bayerischer Wald" is supported by geochronological and geotectonic similarities with the Habach terrane (Tauern Window; Eichhorn et al., 2001); the latter is part of the pre-Variscan basement of the Alps (proto-Alps), which can be seen as the "eastern" extension of the peri-Gondwana terranes (Schätz et al., 2002; Tait et al., 2000; von Raumer et al., 2002).

Summary

The Th-U chemistry of different internal zircon structures identified by CL imaging in this study suggests that Th/U ratios of magmatic zircon tend to be higher than values generally accepted as the lower limit of magmatic values (Th/U >0.3; Rubatto et al., 2001; Schaltegger et al., 1999; Vavra et al., 1999), consistent with values (Th/U >0.5) reported by Brown and Fletcher (1999) for non-metamorphic rhyolite zircons. Th/U ratios intermediate between 'magmatic' and 'metamorphic' values (0.5–0.1) indicate annaling/recrystallization of originally magmatic zircon. Such zircons usually yield geologically meaningful ages, often identical to ages from magmatic zircon domains.

The investigated zircons from the Moldanubian of the Bayerischer Wald indicate a complex chronology of events at ~ 2.7 Ga, ~ 2.0 Ga, ~ 640 Ma (inherited cores; NE Bayerischer Wald), 550 Ma (magmatism; SW Bayerischer Wald), 490–460 Ma (magmatism, anatexis; NE Bayerischer Wald), 430 Ma (metamorphism; NE Bayerischer Wald) and ~ 320 Ma (metamophism). Palaeoproterozoic-Archaean and Neoproterozoic ages of inherited zircons, as well as Nd model ages ranging from 1.18–1.65 Ga interpreted to reflect mixing of recycled and juvenile crust suggest a Gondwana-related origin, probably with affinities to the West African craton. Upper Vendian acid and basic magmatism in the south-western part of the Bayerischer Wald took place at an active continental margin with ensialic back arc development. Lower Ordovician magmatism, evidenced in the north-eastern parts, is more heterogeneous with continental- and subduction-related metagranitoids and metarhyolites, leucosomes, andesitic and tectonically-emplaced MORB-type metabasites. An active continental margin setting, possibly with some lateral variation (accretion/collision) similar to the North American active margin (Patchett and

Chase, 2002) is envisaged for the Lower Ordovician magmatism. MORB-type metabasites seem to be related to ZEV and Mariánské Lázně Complex metabasites representing the products of continental or oceanic rifting (O'Brien et al., 1997). Convergent conditions in the Upper Vendian and Lower Ordovician favour a position of the "Bayerischer Wald" in the "eastern" prolongation of terranes of the northern Gondwana margin, probably in close relation to the Habach terrane (proto-Alps; Eichhorn et al., 2001) as suggested by geochronological and geodynamic similarities.

Acknowledgements Zircon preparation and CL imaging were performed at the Department für Geo- und Umweltwissenschaften (Ludwig-Maximilians-Universität München). Zircon analyses for six samples were carried out on the sensitive high-resolution ion microprobe (SHRIMP II) in Perth during a measurement campaign by U.T. and R.E. in 2001; one sample was analyzed at the SHRIMP II by R.E. and G.L. in 1998. SHRIMP II is operated by a consortium consisting of the Curtin University of Technology, the University of Western Australia, and the Geological Survey of Western Australia, with the support of the Australian Research Council. We would like to thank Stefan Wamsler for providing one of the metabasite samples. We are indebted to Eckhardt Stein, Wolfgang Dörr and an anonymous reviewer for their critical and constructive comments. We gratefully acknowledge financial support of Graf von Thun und Hohenstein (München), President Hubert Schmid of the Bavarian Geological Survey (München) and the Bayerisches Staatsministerium für Umwelt, Gesundheit und Verbraucherschutz (München) for SHRIMP dating in 2001, and of the Deutsche Forschungsgemeinschaft (DFG) for SHRIMP dating in 1998 (Ho 488/23–1) and for isotope analyses (Ho 488/24–1).

References

Arndt, NT, Goldstein, SL (1987) Use and abuse of crust-formation ages. Geology 15:893–895

Bauberger, W (1977) Geologische Karte von Bayern, 1:25000, Erläuterungen zum Blatt Nr. 7046 Spiegelau und zum Blatt Nr. 7047 Finsterau sowie zu den nördlichen Anteilen der Blätter Nr. 7146 Grafenau und Nr. 7147 Freyung, Nationalpark Bayerischer Wald. Bayer Geol Landesamt, München, 183 pp

Bauberger, W, Unger, HJ (1984) Geologische Karte von Bayern, 1:25000, Erläuterungen zum Blatt Nr. 7446 Passau. Bayer Geol Landesamt, München, 175 pp

Bayer Geol Landesamt (1996) Geologische Karte von Bayern - 1:500 000. Bayer Geol Landesamt, München

Blümel, P (1972) Die Analyse von Kristallisation und Deformation einer metamorphen Zonenfolge im Moldanubikum von Lam-Bodenmais, E-Bayern. N Jahrb Mineral Abh 118:74–96

Blümel, P, Schreyer, W (1977) Phase relations in pelitic and psammitic gneisses of the sillimanite-potash feldspar and cordierite-potash feldspar zones in the Moldanubicum of the Lam-Bodenmais area, Bavaria. J Petrol 18:431–459

Bowes, DR, Aftalion, M (1991) U-Pb zircon isotopic evidence for early Ordovician and late Proterozoic units in the Marianske Lazne complex, Central European Hercynides. N Jahrb Mineral Mh 7:315–326

Brown, SJA, Fletcher, IR (1999) SHRIMP U-Pb dating of the preeruption growth history of zircons from the 340 ka Whakamaru Ignimbrite, New Zealand: Evidence for >250 k.y. magma residence times. Geology 27:1035–1038

Bues, C, Dörr, W, Fiala, J, Vejnar, Z, Zulauf, G (2002) Emplacement depths and radiometric ages of Paleozoic plutons of the Neukirchen-Kdyne massif: differential uplift and exhumation of Cadomian basement due to Carboniferous orogenic collapse (Bohemian Massif). Tectonophysics 352:225–243

Chen, F, Hegner, E, Todt, W (2000) Zircon ages and Nd isotopic and chemical compositions of orthogneisses from the Black Forest, Germany: evidence for a Cambrian magmatic arc. Int J Earth Sci 88:791–802

Chen, F, Todt, W, Hann, HP (2003) Zircon and Garnet Geochronology of Eclogites from the Moldanubian Zone of the Black Forest, Germany. J Geol 111:207–222

Claoué-Long, JC, Compston, W, Roberts, J, Fanning, CM (1995) Two Carboniferous ages: a comparison of SHRIMP zircon dating with conventional zircon ages and $^{40}Ar/^{39}Ar$ analyses. SEPM Spec Publ 54:3-21

Compston, W, Williams, IS, Meyer, C (1984) U-Pb geochronology of zircons from lunar breccia 73217 using a sensitive high-resolution ion-microprobe. J Geophys Res 89:525–534

Dörr, W, Zulauf, G, Fiala, J, Franke, W, Vejnar, Z (2002) Neoproterozoic to Early Cambrian history of an active plate margin in the Teplá-Barrandian unit—a correlation of U-Pb isotopic-dilution-TIMS ages (Bohemia, Czech Republic). Tectonophysics 352:65–85

Düsing, C (1959) Geologische Karte von Bayern 1:25 000, Erläuterungen zum Blatt 6540 Oberviechtach. Bayer Geol Landesamt, München, 90 pp

Eichhorn, R, Höll, R, Loth, G, Kennedy, A (1999) Implications of U-Pb SHRIMP zircon data on the age of the Felbertal tungsten deposit (Tauern Window, Austria). Int J Earth Sci 88:496–512

Eichhorn, R, Loth, G, Kennedy, A (2001) Unravelling the pre-Variscan evolution of the Habach terrane (Tauern Window, Austria) by U-Pb SHRIMP zircon data. Contrib Mineral Petrol 142:147–162

Fernández-Suárez, J, Gutiérrez-Alonso, G, Jeffries, TE (2002) The importance of along-margin terrane transport in northern Gondwana: insights from detrital zircon parentage in Neoproterozoic rocks from Iberia and Brittany. Earth Planet Sci Lett 204:75–88

Franke, W (1989) Tectonostratigraphic units in the Variscan belt of central Europe. Geol Soc Am Spec Pap 230:67–90

Franke, W, Dallmeyer, RD, Weber, K (1995) Geodynamic evolution. In: Dallmeyer, RD, Franke, W, Weber, K (eds) Pre-Permian Geology of central and eastern Europe. Springer, Berlin, pp 579–593

Friedl, G (2000) Deducing the ancestry of terranes: SHRIMP evidence for South America-derived Gondwana fragments in central Europe. Geology 28:1035–1038

Gebauer, D, Williams, IS, Compston, W, Grünenfelder, M (1989) The development of the central European continental crust since the Early Archean based on conventional and ion-microprobe dating of up to 3.84 b.y. old detrital zircons. Tectonophysics 157:81–96

Gradstein, FM, Ogg, J (1996) A Phanerozoic time scale. Episodes 19:3-5

Grauert, B, Hänny, R, Soptrajanova, G (1973) Age and origin of detrital zircons from the pre-Permian basements of the Bohemian Massif and the Alps. Contrib Mineral Petrol 40:105–130

Grauert, B, Hänny, R, Soptrajanova, G (1974) Geochronology of a polymetamorphic and anatectic gneiss region: the Moldanubicum of the area Lam-Deggendorf, Eastern Bavaria, Germany. Contrib Mineral Petrol 45:37–63

Heaman, LM, Bowins, R, Crocket, J (1990) The chemical composition of igneous zircon suites: implications for geochemical tracer studies. Geochim Cosmochim Acta 54:1597–1607

Hegner, E, Kröner, A (2001) Review of Nd isotopic data and xenocrystic and detrital zircon ages from the pre-Variscan basement in the eastern Bohemian Massif: speculations on palinspastic reconstructions. In: Franke, W, Haal, V, Oncken, O, Tanner, D (eds) Orogenic processes: Quantification and Modelling in the Variscan Belt. Geol Soc London, Spec Publ 179, London, pp 113–129

Ihlenfeld, C, Rohrmüller, J, Köhler, H (1998) The Teplá-Barrandian/Moldanubian boundary: isotopic investigations on rocks and minerals from the Rittsteig drilling (NE-Bavaria, Ger-

many). In: Novak, M, Rosenbaum, J (eds) Challenges to chemical geology. Czech Geol Survey, Praha, pp 69–92
Kalt, A, Berger, A, Blümel, P (1999) Metamorphic evolution of cordierite-bearing migmatites from the Bayerische Wald (Variscan Belt, Germany). J Petrol 40:601–627
Kalt, A, Corfu, F, Wijbrams, JR (2000) Time calibration of a P-T path from a Variscan high-temperature low-pressure metamorphic complex (Bayerische Wald, Germany), and the detection of inherited monazite. Contrib Mineral Petrol 138:143–163
Kemnitz, H, Romer, RL, Oncken, O (2002) Gondwana break-up and the northern margin of the Saxothuringian belt (Variscides of Central Europe). Int J Earth Sci 91:246–259
Kennedy, AK (2000) The Search for New Zircon Standards for SIMS. Abstract volume AGC New Frontiers Conference: 109–111
Köhler, H, Propach, G, Troll, G (1989) Exkursion zur Geologie, Petrographie und Geochronologie des NE-bayerischen Grundgebirges. Eur J Mineral 1(Bh. 2): 1–84
Kröner, A, Hegner, E (1998) Geochemistry, single zircon ages and Sm-Nd systematics of granitoid rocks from the Góry Sowie (Owl Mts.), Polish West Sudetes: evidence for early Palaeozoic arc-related plutonism. J Geol Soc London 155:711–724
Kröner, A, Jaeckel, P, Hegner, E, Opletal, M (2001) Single zircon ages and whole-rock Nd isotopic systematics of early Palaeozoic granitoid gneisses from the Czech and Polish Sudetes (Jizerské hory, Krkonose Mountains and Orlice-Snezník Complex). Int J Earth Sci 90:304–324
Kröner, A, Wendt, I, Liew, TC, Compston, W, Todt, W, Fiala, J, Vankova, V, Vanek, J (1988) U-Pb zircon and Sm-Nd model ages of high-grade Moldanubian metasediments, Bohemian Massif, Czechoslovakia. Contrib Mineral Petrol 99:257–266
Kröner, A, Willner, AP (1998) Time of formation and peak of Variscan HP-HT metamorphism of quartz-feldspar rocks in the central Erzgebirge, Saxony, Germany. Contrib Mineral Petrol 132:1-20
Kröner, A, Willner, AP, Hegner, E, Frischbutter, A, Hofmann, J, Bergner, R (1995) Latest Precambrian (Cadomian) zircon ages, Nd isotopic systematics and P-T evolution of granitoid orthogneisses of the Erzgebirge, Saxony and Czech Republic. Geol Rundsch 84:437–456
Liew, TC, Hofmann, AW (1988) Precambrian crustal components, plutonic associations, plate environment of the Hercynian Fold Belt of central Europe: indications from a Nd and Sr isotopic study. Contrib Mineral Petrol 98:129–138
Linnemann, U, Gehmlich, M, Tichomirowa, M, Buschmann, B, Nasdala, L, Jonas, P, Lützner, H, Bombach, K (2000) From Cadomian subduction to Early Palaeozoic rifting: the evolution of Saxo-Thuringia at the margin of Gondwana in the light of single zircon geochronology and basin development (Central European Variscides, Germany). In: Franke, W, Haak, V, Oncken, O, Tanner, D (eds) Orogenic processes: Quantification and modelling in the Variscan Belt. Geol Soc London, Spec Publ 179, London, pp 131–153
Loth, G, Eichhorn, R, Höll, R, Kennedy, A, Schauder, P, Söllner, F (2001) Cambro-Ordovician age of a metagabbro from the Wildschönau ophiolite complex, Greywacke Supergroup (Eastern Alps, Austria): a U-Pb SHRIMP study. Eur J Mineral 13:57–66
Ludwig, KR (2001) User's manual for Isoplot /Ex rev. 2.49 - a geochronological toolkit for Microsoft Excel. Berkeley Geochronol Center Spec Publ 1a: 1–55
McLaren, AC, FitzGerald, JD, Williams, IS (1994) The microstructure of zircon and its influence on the age determination from Pb/U isotopic ratios measured by ion microprobe. Geochim Cosmochim Acta 58:993–1005
Mielke, H (1990) Geologische Karte von Bayern, 1:25000, Erläuterungen zum Blatt Nr. 6542 Untergrafenried und zum Blatt Nr. 6642 Waldmünchen. Bayer Geol Landesamt, München, 95 pp
Mielke, H (2002) Geologische Karte von Bayern, 1:25000, Erläuterungen zum Blatt Nr. 6641 Rötz. Bayer Geol Landesamt, München, 119 pp
Mielke, H, Rohrmüller, J, Gebauer, D (1996) Ein metalateritisches Denudations-Niveau als lithologisch und zeitlich korrelierbarer Bezugshorizont in Phylliten, Glimmerschiefern und Gneisen des ostbayerischen Grundgebirges. Geol Bav 101:139–166
Mingram, B (1998) The Erzgebirge, Germany, a subducted part of northern Gondwana: geochemical evidence for repetition of early Palaeozoic metasedimentary sequences in metamorphic thrust units. Geol Mag 135:785–801
Möller, A, O'Brien, PJ, Kennedy, A, Kröner, A (2002) Polyphase zircon in ultrahigh-temperature granulites (Rogaland, SW Norway): constraints for Pb diffusion in zircon. J Metam Geol 20:727–740
Murphy, JB, Strachan, RA, Nance, RD, Parker, KD, Fowler, MB (2000) Proto-Avalonia: A 1.2–1.0 Ga tectonothermal event and constraints for the evolution of Rodinia. Geology 28:1071–1074
Nance, RD, Murphy, JB (1996) Basement isotopic signatures and Neoproterozoic paleogeography of Avalonian-Cadomian and related terranes in the circum-North Atlantic. Geol Soc Am Spec Pap 304:333–346
Nance, RD, Murphy, JB, Keppie, JD (2002) A Cordilleran model for the evolution of Avalonia. Tectonophysics 352:11–31
Nance, RD, Murphy, JB, Strachan, RA, D'Lemos, RS, Taylor, GK (1991) Late Proterozoic tectonostratigraphic evolution of the Avalonian and Cadomian terranes. Precambrian Res 53:41–78
Nemchin, AA, Pidgeon, RT (1997) Evolution of the Darling Range Batholith, Yilgarn Craton, Western Australia: a SHRIMP zircon study. J Petrol 38:625–649
O'Brien, PJ (1989a) The petrology of eclogites and related rocks from the Bavarian margin of the Bohemian Massif, West Germany. Unpubl PhD Thesis, University of Sheffield
O'Brien, PJ (1989b) The petrology of retrograded eclogites of the Oberpfalz Forest, northeastern Bavaria, West Germany. Tectonophysics 157:195–212
O'Brien, PJ, Duyster, J, Grauert, B, Schreyer, W, Stöckhert, B, Weber, K (1997) Crustal evolution of the KTB drill site: From oldest relics to the late Hercynian granites. J Geophys Res 102:18203–18220
O'Nions, RK, Hamilton, PJ, Evensen, NM (1977) Variations in $^{143}Nd/^{144}Nd$ and $^{87}Sr/^{86}Sr$ in oceanic basalts. Earth Planet Sci Lett 34:13–22
Ott, W-D (1988) Geologische Karte von Bayern, 1:25000, Erläuterungen zum Blatt Nr. 7147 Freyung und zum Blatt Nr. 7148 Bischofsreut. Bayer Geol Landesamt, München, 136 pp
Patchett, PJ, Chase, CG (2002) Role of transform continental margins in major crustal growth episodes. Geology 30:39–42
Pidgeon, RT (1992) Recrystallization of oscillatory zoned zircon: some geochronological and petrological implications. Contrib Mineral Petrol 110:463–472
Pidgeon, RT (1997) Gem zircon: a new role as a standard for the measurement of geological time using ion microprobes. Z Dtsch Gemmol Ges 46: 21–28
Pidgeon, RT, Nemchin, AA, Hitchen, GJ (1998) Internal structures of zircons from Archaean granites from the Darling Range batholith: implications for zircon stability and the interpretation of zircon U-Pb ages. Contrib Mineral Petrol 132:288–299
Pin, C, Lancelot, J (1982) U-Pb dating of an Early Palaeozoic bimodal magmatism in the French Massif Central and of its further metamorphic evolution. Contrib Mineral Petrol 79:1-12
Pin, C, Marini, F (1993) Early Ordovician continental break-up in Variscan Europe: Nd-Sr isotope and trace element evidence from bimodal igneous associations of the southern Massif Central, France. Lithos 29:177–196
Pin, C, Paquette, J-L (1997) A mantle-derived bimodal suite in the Hercynian Belt: Nd isotope and trace element evidence for a subduction-related rift origin of the Late Devonian Brévenne metavolcanics, Massif Central (France). Contrib Mineral Petrol 129:222–238

Propach, G, Baumann, A, Schulz-Schmalschläger, M, Grauert, B (2000) Zircon and monazite U-Pb ages of Variscan granitoid rocks and gneisses in the Moldanubian zone of eastern Bavaria, Germany. N Jahrb Geol Paläont Mh 2000(6): 345–377

Remane, J, Faure-Muret, A, Odin, GS (2000) International stratigraphic chart. IUGS

Rohrmüller, J, Mielke, H, Gebauer, D (1996) Gesteinsfolge des Grundgebirges nördlich der Donau und im Molasseuntergrund. In: Bayer Geol Landesamt (ed) Erläuterungen zur Geologischen Karte von Bayern, 1:500000. Bayer Geol Landesamt, München, pp 16–54

Rubatto, D (2002) Zircon trace element geochemistry: partitioning with garnet and the link between U–Pb ages and metamorphism. Chem Geol 184:123–138

Rubatto, D, Gebauer, D, Compagnoni, R (1999) Dating of eclogite-facies zircons: the age of Alpine metamorphism in the Sesia–Lanzo Zone (Western Alps). Earth Planet Sci Lett 167:141–158

Rubatto, D, Williams, IS, Buick, IS (2001) Zircon and monazite response to prograde metamorphism in the Reynolds Range, central Australia. Contrib Mineral Petrol 140:458–468

Schaltegger, U, Fanning, CM, Günther, D, Maurin, JC, Schulmann, K, Gebauer, D (1999) Growth, annealing and recrystallization of zircon and preservation of monazite in high-grade metamorphism: conventional and in-situ U-Pb isotope, cathodoluminescence and microchemical evidence. Contrib Mineral Petrol 134:186-201

Schaltegger, U, Nägler, TF, Corfu, F, Maggetti, M, Galetti, G, Stosch, HG (1997) A Cambrian island arc in the Silvretta nappe: constraints from geochemistry and geochronology. Schweiz Mineral Petrogr Mitt 77:337–350

Schätz, M, Reischmann, T, Tait, J, Bachtadse, V, Bahlburg, H, Martin, U (2002) The Early Palaeozoic break-up of northern Gondwana, new palaeomagnetic and geochronological data from the Saxothuringian Basin, Germany. Int J Earth Sci 91:838–849

Schauder, P (2002) Ordovizische Entwicklungen im Westabschnitt der Nördlichen Grauwackenzone unter besonderer Berücksichtigung mafischer und ultramafischer Magmatite. Geochemische, isotopengeochemische und geochronologische Untersuchungen. Münchner Geol Hefte A30:1-103

Schuster, J (1994) Metamorphic evolution of the Moldanubian zone of the Oberpfälzer Wald/NE Bavaria. J Czech Geol Soc 39:99

Siebel, W, Chen, F, Satir, M (2003) Late-Variscan magmatism revisited: new implications from Pb-evaporation zircon ages on the emplacement of redwitzites and granites in NE Bavaria. Int J Earth Sci 92:36–53

Söllner, F, Nelson, DR, Miller, H (1997) Provenance, deposition and age of gneiss units from the KTB drill hole (Germany): evidence from SHRIMP and conventional U-Pb zircon age determinations. Geol Rundsch 86(Suppl): S235-S250

Steiger, RH, Jäger, E (1977) Subcommission on geochronology: convention of the use of decay constants in geo- and cosmochronology. Earth Planet Sci Lett 36:359–362

Tait, J, Schätz, M, Bachtadse, V, Soffel, H (2000) Palaeomagnetism and Palaeozoic palaeogeography of Gondwana and European terranes. In: Franke, W, Haak, V, Oncken, O, Tanner, D (eds) Orogenic processes: Quantification and modelling in the Variscan Belt. Geol Soc London, Spec Publ 179, London, pp 21–32

Tait, JA, Bachtadse, V, Franke, W, Soffel, HC (1997) Geodynamic evolution of the European Variscan fold belt: palaeomagnetic and geological constraints. Geol Rundsch 86:585–598

Tanner, DC, Schuster, J, Behrmann, JH, O'Brien, PJ (1993) New clues to the Moldanubian puzzle: structural and petrological observations from the Waldmünchen area, eastern Bavaria. KTB-Report 93–2: 97–102

Teipel, U (2003) Obervendischer und unterordovizischer Magmatismus im Bayerischen Wald—Geochronologische (SHRIMP), geochemische und isotopengeochemische Untersuchungen an Metamagmatiten aus dem Westteil des Böhmischen Massivs. Münchner Geol Hefte A33:1-98

Teufel, S (1988) Vergleichende U-Pb- und Rb-Sr-Altersbestimmungen an Gesteinen des Übergangsbereichs Saxothuringikum/Moldanubikum, NE-Bayern. Göttinger Arb Geol Paläont 35:1-87

Troll, G (1967) Führer zu geologisch-petrographischen Exkursionen im Bayerischen Wald. Teil1: Aufschlüsse im Mittel- und Ostteil. Geol Bav 58

Troll, G, Linhardt, TE, Skeries, R (1987) Petrographic and geochemical studies on country rock of the Bodenmais (Bavaria) sulphide deposit. N Jahrb Geol Paläont Mh 1987:726–752

van Staal, CR, Dewey, JF, Mac Niocaill, C, McKerrow, WS (1998) The Cambrian–Silurian tectonic evolution of the Northern Appalachians and British Caledonides; history of a complex, west and southwest Pacific-type segment of Iapetus. In: Blundell, D, Scott, AC (eds) Lyell: The Past is the Key to the Present. Geol Soc London Spec Publ, London, pp 199– 242

Vavra, G, Gebauer, D, Schmid, R, Compston, W (1996) Multiple zircon growth and recrystallization during polyphase Late Carboniferous to Triassic metamorphism in granulites of the Ivrea Zone (Southern Alps): an ion microprobe (SHRIMP) study. Contrib Mineral Petrol 122:337–358

Vavra, G, Schmid, R, Gebauer, D (1999) Internal morphology, habit and U-Th-Pb microanalysis of amphibolite-to-granulite facies zircons: geochronology of the Ivrea Zone (Southern Alps). Contrib Mineral Petrol 134:380–404

von Quadt, A (1997) U-Pb zircon and Sr-Nd-Pb whole-rock investigations from the continental deep drilling (KTB). Geol Rundsch 86(Suppl): S258-S271

von Quadt, A, Gebauer, D (1993) Sm-Nd an U-Pb dating of eclogites and granulites from the Oberpfalz, NE Bavaria, Germany. Chem Geol 109:317–339

von Raumer, JF, Stampfli, GM, Borel, G, Bussy, F (2002) Organization of pre-Variscan basement areas at the north-Gondwana margin. Int J Earth Sci 91:35–52

Wasserburg, GJ, Jacobsen, SB, DePaolo, DJ, McCulloch, MT (1981) Precise determination of Sm/Nd ratios, Sm and Nd isotopic abundances in standard solutions. Geochim Cosmochim Acta 45:2311–2323

Webby, BD, Cooper, RA, Bergström, SM, Paris, F (2001) Ordovician time scale; an introduction. In: Holroyd, PA (ed) IGCP Project No. 410; The Great Ordovician Biodiversification event. Paleo Bios, pp 13–14

Wendt, I, Kröner, A, Fiala, J, Todt, W (1993) Evidence from zircon dating for existence of approximately 2.1 Ga old crystalline basement in southern Bohemia, Czech Republic. Geol Rundsch 82:42–50

Williams, IS (2001) Response of detrital zircon and monazite, and their U–Pb isotopic systems, to regional metamorphism and host-rock partial melting, Cooma Complex, southeastern Australia. Australian J Earth Sci 48:557–580

Williams, IS, Buick, IS, Cartright, I (1996) An extended episode of early Mesoproterozoic metamorphic fluid flow in the Reynolds Range, central Australia. J Metam Geol 14:29–47

Zulauf, G, Dörr, W, Fiala, J, Vejnar, Z (1997) Late Cadomian crustal tilting and Cambrian transtension in the Teplá-Barrandian unit (Bohemian Massif, Central European Variscides). Geol Rundsch 86:571–584

Zulauf, G, Schitter, F, Riegler, G, Finger, F, Fiala, J, Vejnar, Z (1999) Age constraints on the Cadomian evolution of the Teplá-Barrandian unit (Bohemian Massif) through electron microprobe dating of metamorphic monazite. Z Dtsch Geol Ges 150:627–639